Green Chemistry

ROYAL SOCIETY OF CHEMISTRY

CRITICAL REVIEW

View Article Online
View Journal | View Issue



Cite this: *Green Chem.*, 2020, **22**, 6258

# Plasma-driven catalysis: green ammonia synthesis with intermittent electricity

Kevin H. R. Rouwenhorst, *[a] Yannick Engelmann,[b] Kevin van 't Veer,[b,c] Rolf S. Postma,[a] Annemie Bogaerts *[b] and Leon Lefferts *[a]

Ammonia is one of the most produced chemicals, mainly synthesized from fossil fuels for fertilizer applications. Furthermore, ammonia may be one of the energy carriers of the future, when it is produced from renewable electricity. This has spurred research on alternative technologies for green ammonia production. Research on plasma-driven ammonia synthesis has recently gained traction in academic literature. In the current review, we summarize the literature on plasma-driven ammonia synthesis. We distinguish between mechanisms for ammonia synthesis in the presence of a plasma, with and without a catalyst, for different plasma conditions. Strategies for catalyst design are discussed, as well as the current understanding regarding the potential plasma-catalyst synergies as function of the plasma conditions and their implications on energy efficiency. Finally, we discuss the limitations in currently reported models and experiments, as an outlook for research opportunities for further unravelling the complexities of plasma-catalytic ammonia synthesis, in order to bridge the gap between the currently reported models and experimental results.

Received 17th June 2020,
Accepted 8th September 2020

DOI: 10.1039/d0gc02058c

rsc.li/greenchem



## 1. Introduction – the need for electrification and energy storage

Renewable energy sources, such as wind energy and solar power, increasingly penetrate the electrical power grid, spurring the electrification of the energy landscape.[1] However, these energy sources are intermittent and energy storage is required. For short-term energy storage (up to a few days), a wide range of technologies is available, including batteries and thermo-mechanical storage.[2] In contrast, chemical energy storage is one of the few alternatives for long-term, seasonal energy storage,[2,3] the other main option being pumped hydropower.[4] Even though pumped hydropower may be a potential solution for low-cost energy storage in some naturally suited areas,[4] the energy density of such systems is low, and pumped hydropower heavily depends on the availability of large natural water formations.

Chemical energy storage in the form of hydrogen is often proposed to solve the intermittency challenge. Hydrogen can be produced from water *via* electrolysis using renewable electricity, producing oxygen as a by-product. Hydrogen can be combusted to water in a fuel cell or gas turbine, producing electricity again. However, hydrogen is not easily stored over longer timespans due to temperature fluctuations over the different seasons, considering the severe storage conditions. Therefore, hydrogen carriers are required and ammonia is one of the options available.[3,5] Ammonia can be used for stationary energy storage, as well as for fuel applications.[3,6,7] Ammonia is a carbon-free hydrogen carrier, which can be produced from air and water. The current ammonia supply accounts for about 170 Mt per year.

Currently, ammonia ($NH_3$) is produced mostly as a synthetic fertilizer *via* thermochemical conversion of hydrogen ($H_2$) and nitrogen ($N_2$), which is crucial to produce sufficient food *via* agriculture to sustain the current world population of almost 8 billion people.[8,9] Hydrogen for this purpose is mostly produced *via* steam reforming of methane, contributing significantly to global warming caused by emission of $CO_2$. Alternative methods to produce ammonia are being researched, both for the purpose of energy storage and/or fertilizer production by using electrical power rather than fossil energy carriers like methane. The goal of this review is to put one specific solution, *i.e.* plasma-catalytic synthesis of ammonia, in perspective of existing and other innovative routes. The reader is introduced to the concepts of plasma chemistry and plasma catalysis, followed by the state of the art of plasma-driven ammonia synthesis.

[a]*Catalytic Processes & Materials, MESA+ Institute for Nanotechnology, University of Twente, P.O. Box 217, 7500 AE Enschede, The Netherlands.*
*E-mail: k.h.r.rouwenhorst@utwente.nl, l.lefferts@utwente.nl*
[b]*Research Group PLASMANT, Department of Chemistry, University of Antwerp, Universiteitsplein 1, B-2610 Wilrijk-Antwerp, Belgium.*
*E-mail: annemie.bogaerts@uantwerpen.be*
[c]*Chemistry of Surfaces, Interfaces and Nanomaterials, Faculty of Sciences, Université Libre de Bruxelles, CP255, Avenue F. D. Roosevelt 50, B-1050 Brussels, Belgium*

## 2. Ammonia synthesis processes

We discuss the current ammonia synthesis processes and non-conventional technologies, starting with the industrial Haber–Bosch process and its modifications for greener ammonia production at milder conditions, after which sustainable and novel ammonia synthesis methods are presented, such as electrochemical, photochemical and homogeneous ammonia synthesis, as well as chemical looping approaches. This provides the background for the core of this review: plasma-driven ammonia synthesis.

### 2.1. The Haber–Bosch process

This section serves as an introduction to commercial ammonia synthesis processes *via* the Haber–Bosch process. We present the basics of the hydrogen production, nitrogen production, and ammonia synthesis loop. Conventional ammonia production processes are extensively discussed in ref. 10–13. We also elaborate on scale-down and intermittency issues,[6] providing a rationale for research on novel technologies.

**2.1.1. Brief history of the Haber–Bosch process.** The Haber–Bosch process was developed in the early 20$^{th}$ century as the first industrial large-scale process for fixating nitrogen in the form of ammonia.[11,14] In 1908, the chemist Fritsch Haber and his co-worker Robert Le Rossignol demonstrated that the ammonia synthesis reaction from nitrogen and hydrogen was industrially viable.[15] Using Le Châtelier's principle, they found that significantly increasing the pressure shifts the equilibrium of the reaction towards the product side (eqn (1)).

$$3H_2 + N_2 \rightleftharpoons 2NH_3 \text{ with } \Delta H_r^\circ = -91.8 \text{ kJ mol}^{-1} \quad (1)$$

The high-pressure, industrial ammonia synthesis process was developed by Carl Bosch and co-workers. The first plant in Oppau (Germany) was operational by 1913, with a production capacity of 30 t-$NH_3$ d$^{-1}$. Since then, the Haber–Bosch process and catalysts have undergone only gradual changes.[11,12] Hydrogen and nitrogen react in a $H_2:N_2$ molar ratio of 2 : 1 to 3 : 1 over a multiple-promoted iron catalyst at 400–500 °C and 100–450 bar.[16] The Haber–Bosch process has outcompeted other nitrogen fixation processes, such as $NO_x$ production using electrical arcs (the Birkeland–Eyde process)[17,18] and the cyanamide process (the Frank–Caro process).[18,19] The development and evolution of nitrogen fixation processes is shown in Fig. 1, from which it follows that the best Haber–Bosch plants have energy consumptions close to the lower heating value of 18.6 GJ t-$NH_3^{-1}$.

**2.1.2. Process description.** Nearly all ammonia is currently produced from fossil fuels, such as natural gas, naphtha, heavy fuel oil, and coal.[14,21] This ammonia is termed *brown* ammonia, while ammonia produced from fossil fuels with carbon capture and storage (CCS) is termed *blue* ammonia. Ammonia produced with essentially zero carbon footprint from electrolysis-based or biomass-based hydrogen is termed *green* ammonia. A process flow diagram of a steam methane reforming-based Haber–Bosch process is shown in Fig. 2.

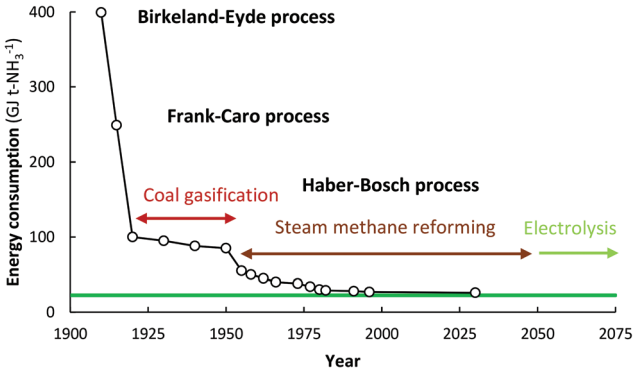


**Fig. 1** Energy consumption of synthetic nitrogen fixation processes, and the theoretical minimum energy consumption (green line). Adapted and modified from ref. 20.

The ammonia production process starts with hydrogen production, usually through stream methane reforming (SMR), with >70% of the ammonia currently produced (eqn (2)).[11,12,21] Other processes for hydrogen production include coal or biomass gasification and electrolysis.[14,20] In the primary reforming section (the tubular reformer), natural gas and water react at 400–800 °C. Nitrogen is usually introduced by adding air at the second stage of the reforming process (the autothermal reformer), in which part of the oxygen is burned to overcome the endothermicity of the steam methane reforming reaction.[11] In both reforming stages, a nickel-based catalyst is used. The residual $CH_4$ concentration is below 0.5 vol%.[12]

$$CH_4 + H_2O \rightleftharpoons CO + 3H_2 \text{ with } \Delta H_r^\circ = 206 \text{ kJ mol}^{-1} \quad (2)$$

$$CO + H_2O \rightleftharpoons CO_2 + H_2 \text{ with } \Delta H_r^\circ = -41.1 \text{ kJ mol}^{-1} \quad (3)$$

Subsequently, the produced gas mixture is subjected to a series of water gas shift (WGS) reactors to maximize the hydrogen yield and to remove the bulk of CO present in the gas stream (eqn (3)). A decrease in temperature is favoured to push the conversion to $H_2$ and $CO_2$ production, due to the exothermicity of the reaction. A two-stage shift conversion is usually applied to optimize the efficiency of the reactor and catalyst usage. First, the gas mixture is fed to a high-temperature-shift catalyst bed of $Fe_2O_3/Cr_2O_3$ at 350–400 °C, after which the gas mixture is fed to a low-temperature-shift catalyst bed of $CuO/ZnO/Al_2O_3$ at 200–220 °C.[23] The residual CO concentration after the low-temperature-shift reactor is below 0.3 vol%.[12]

Gas cleaning is required before ammonia synthesis. Firstly, the $CO_2$ is scrubbed out using a caustic scrub, either based on amines like MEA or MDEA, or alkali hydroxides like potash.[11,12] The added benefit is that any remaining sulfur or nitrous oxide compounds are also removed. Secondly, any remaining CO is reactively removed through methanation (reverse of eqn (2)) at 250–350 °C and 25 bar, using a nickel catalyst.[12]

Alternative methods for nitrogen generation include cryogenic air separation, pressure swing adsorption, and membrane permeation.[11,24,25] While cryogenic air separation is

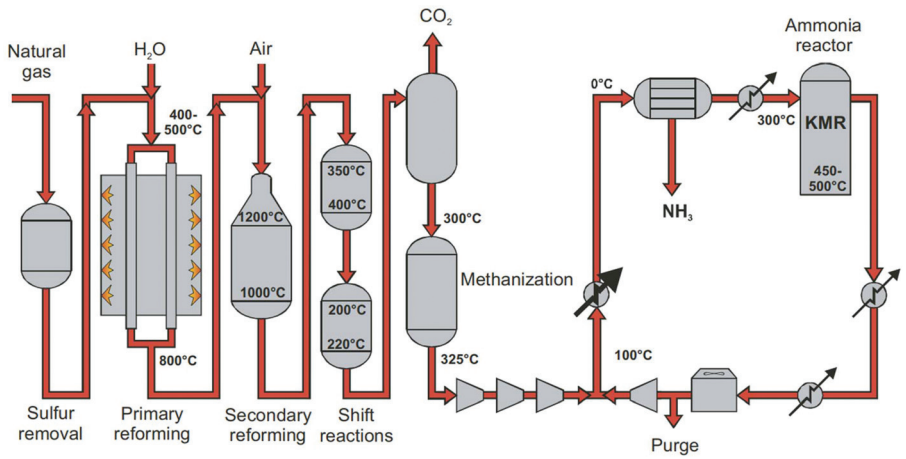


Fig. 2 Process flow diagram of steam methane reforming-based Haber–Bosch process. KMR is a commercial multiple promoted iron-based ammonia synthesis catalyst. Reproduced from ref. 22.

usually the preferred technology at industrial scale, small-scale operation may be facilitated by nitrogen production by pressure swing adsorption.[6,25]

After gas purification, the reaction mixture is compressed to 100–450 bar for the ammonia synthesis loop (see Fig. 2). High temperature (400–500 °C) is required because of the limited activity of the iron catalyst for breaking the triple nitrogen–nitrogen bond (N≡N), which is the rate-determining step for ammonia synthesis.[26,27] High pressure is required to shift the thermodynamic equilibrium towards ammonia, achieving typically 25 vol% ammonia at the reactor outlet.[10,12] The product mixture is cooled to near-ambient temperatures (−20 °C to 30 °C) to separate the bulk of the produced ammonia from the reaction mixture *via* condensation.[12] The remaining gasses are compressed back up to reaction pressures, mixed with fresh make-up gas and sent back into the reactor. Furthermore, a purge is required in the recycle to prevent the accumulation of inert gases, *i.e.* mainly $CH_4$ and Ar.

**2.1.3. Catalyst.** The catalyst used in the ammonia synthesis loop is arguably one of the most important aspects of the whole process. The activity of the catalyst determines the required operating temperature for the reactor. This determines the operational pressure to achieve sufficient conversion, and consequently the required compression, as well as the cooling requirement for condensation. Also, the catalyst lifetime is an important factor in determining the run time of the process before a new catalyst is required, which is determined by the catalyst resistance to chemical parameters such as poisons and physical parameters in the process such as a high temperature.[11,12]

The most widely used catalyst for ammonia synthesis is a multiple promoted iron-catalyst, containing a mix of $Al_2O_3$, MgO and $SiO_2$ for mechanical strength and as structural promoters, as well as some electronic promoters such as CaO and $K_2O$.[28] Iron-based catalysts typically have a typical lifetime of at least 10 years.[29–31]

Table 1 Reaction mechanism for ammonia synthesis over the industrial iron-catalyst

| | Reaction | Note |
|---|---|---|
| $H_2$ dissociation | $H_2 + 2^* \rightleftharpoons 2H^*$ | |
| $N_2$ dissociation | $N_2 + 2^* \rightleftharpoons 2N^*$ | Rate-determining step |
| Hydrogenation reactions | $N^* + H^* \rightleftharpoons NH^* + *$ | |
| | $NH^* + H^* \rightleftharpoons NH_2^* + *$ | |
| | $NH_2^* + H^* \rightleftharpoons NH_3^* + *$ | |
| $NH_3$ desorption | $NH_3^* \rightleftharpoons NH_3 + *$ | |

The reaction mechanisms for ammonia synthesis from $H_2$ and $N_2$ over the industrial iron-catalyst have been heavily debated over the past century.[32–37] Only in the late 1970s, Ertl *et al.*[33] were able to construct a free energy diagram for gas phase ammonia synthesis and ammonia synthesis over the industrial iron-catalyst. The reaction mechanism for ammonia synthesis is listed in Table 1.

In the 1910s, Mittasch *et al.*[38,39] put a tremendous effort into finding a suitable catalyst for ammonia synthesis by scanning a large part of the periodic table and mixtures thereof. Only decades later, it was consolidated that the binding strength of nitrogen is a descriptor for ammonia synthesis activity.[22] Furthermore, electronic promoters can substantially change the activity by altering the barrier for breaking the triple N≡N bond.[40,41] A so-called volcano curve was developed, with the binding strength of nitrogen as a descriptor for the ammonia synthesis rate (see Fig. 3). Materials that bind nitrogen too strongly (*i.e.*, on the left-hand side of the volcano curve), easily dissociate nitrogen. However, the ammonia is also strongly bound to the surface of these catalysts, causing desorption limitations, or the N-atoms on the surface are too stable, converting slowly to ammonia. On the other hand, materials that bind nitrogen too weakly (*i.e.*, on the right-hand side of the volcano curve), have limitations for nitrogen dissociation due to a high nitrogen dissociation barrier. An optimum is achieved at intermediate binding strength of nitro-

 

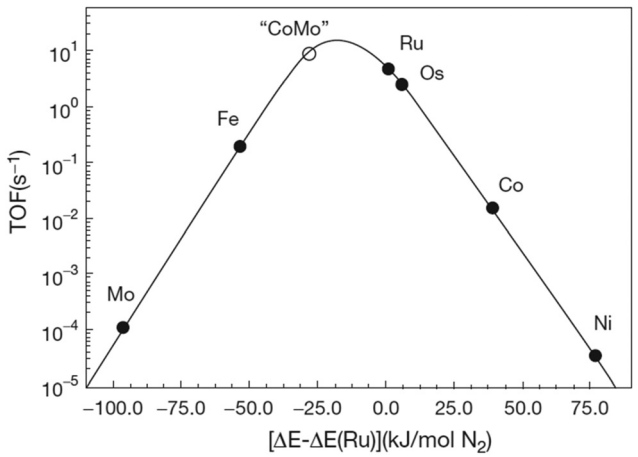


Fig. 3 Calculated turnover frequencies for ammonia synthesis as a function of the adsorption energy of nitrogen (at 400 °C, 50 bar, $H_2 : N_2$ = 3 : 1 and 5% $NH_3$). Reproduced from ref. 47.

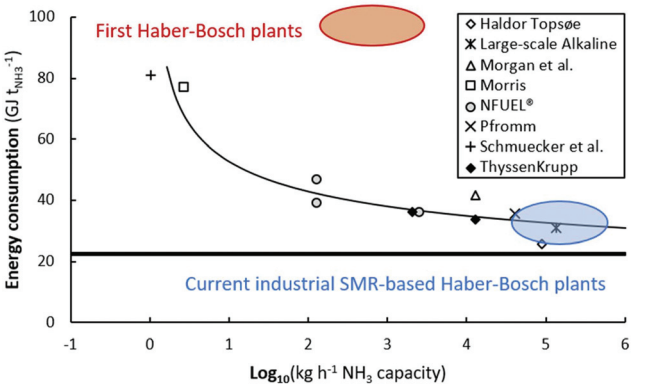


Fig. 4 Energy consumption of various electrolysis-based Haber–Bosch processes (academic and industrial estimates). The bold line represents the thermodynamic minimum energy consumption (20.1 GJ t-$NH_3^{-1}$). 100 kg $h^{-1}$ ammonia corresponds to approximately 1 MW. Original references.[56–65] Reproduced from ref. 20.

gen. As follows from Fig. 3, osmium and ruthenium are more active than iron among metal catalysts.[42–45] Among bimetallic catalysts, CoMo nitrides have also been researched, which show activities similar to ruthenium (Ru) catalysts.[46,47] The latter have been used in various industrial plants,[48] but due to the high cost, these have mostly been replaced by the newest generation of iron-catalysts.[28,31,49] Osmium on the other hand cannot be used because it is highly poisonous. Current research focuses on developing catalysts which break the N≡N bond easily, resulting in hydrogenation of N as the rate determining step on the surface.[44,50,51]

**2.1.4. Scale-down and intermittency.** The current trend for large-scale Haber–Bosch plants is further upscaling for minor improvements in energy consumption and minor gains in the capital expenditures.[52] Even though modern, large-scale Haber–Bosch plants operate at a low energy consumption of 27–36 GJ t-$NH_3^{-1}$ (see Fig. 1) close to the theoretical minimum of 20.1 GJ t-$NH_3^{-1}$, these plants are only feasible for continuous, large-scale production up to 3300 t-$NH_3$ $d^{-1}$ nowadays.[53,54] Large-scale *brown* ammonia production allows for relatively low capital investments per tonne of ammonia produced due to the economy of scale. However, such large-scale plants have limited operational flexibility and decarbonisation of current Haber–Bosch plants with intermittent electricity from solar and wind resources coupled with electrolysers is not straightforward.

Another trend for the conventional technology is downscaling to 3–60 t-$NH_3$ $d^{-1}$ for coupling with electrolysers for hydrogen production, which allows for scaling the technology to the size of wind and solar electricity.[6,55] Furthermore, small-scale plants can be installed more easily, and the ammonia can be produced and used locally, saving transportation costs. However, downscaling leads to an increased cost of ammonia production due to the relatively higher capital expenditure.

Thus, there is a need for operation under milder temperatures and pressures as compared to the current Haber–Bosch process to allow for intermittent operation and lower capital expenditures.[14] Furthermore, Haber–Bosch processes suffer from energy losses upon downscaling below 1 t-$NH_3$ $d^{-1}$,[6] which is due to the high temperatures and temperature fluctuations within the process (see Fig. 4). Alternative technologies may allow for sufficiently energy-efficient ammonia production with a low carbon footprint.[18,66]

## 2.2. Sustainable ammonia synthesis

Ammonia is one of the most produced bulk chemicals, with a high carbon footprint.[14,20] For this reason, ammonia synthesis receives much attention, in the transition towards a more environmentally friendly chemical industry. Making ammonia synthesis more sustainable revolves around two main aspects dictating the process energy consumption: (i) hydrogen production, and (ii) the ammonia synthesis loop, which includes both modifying the Haber–Bosch process and novel ammonia synthesis methods.[20,67] These various aspects are discussed in the next sections. Typically, hydrogen production accounts for 90–95% of the energy consumed for ammonia production. Furthermore, operating ammonia synthesis under milder conditions may allow for scale-down and intermittent operation.[6,68]

**2.2.1. Hydrogen production.** Hydrogen production is a prime candidate for electrification in the chemical industry,[69,70] since it can be produced *via* electrolysis from water at a reasonable efficiency of 70–80%. Historically, electrolysis has been a major production method for hydrogen in ammonia synthesis, second only to coal gasification up till the 1950s–1960s. Afterwards, the emergence of low-cost natural gas decreased the share of hydrogen from electrolysis.

Alkaline electrolysis is the most mature technology[71] and therefore used for producing green hydrogen at large scale (10–100 MWs). On the other hand, proton–exchange membrane (PEM) electrolysis has recently received attention for hydrogen production, due to its ability to follow intermittent electrical loads from renewables such as solar and wind.[71,72]

In terms of production capacity, both electrolysis techniques are comparable. However, PEM electrolyzers currently have a higher capital cost due to the use of noble metals. Energy consumptions of 3.8–6.6 kW h $Nm_{H_2}^{-3}$ are reported for both alkaline electrolyzers and PEM electrolyzers, with a current trend towards lower energy consumption (at elevated pressure).[71,73] A major benefit of PEM is that it can produce hydrogen at up to 200 bar pressure, which alleviates the need for energy intensive hydrogen compression.[72]

Further methods for improving the sustainability of hydrogen production are modification of the conventional technology. Examples include electrical heating during SMR[1,74] and carbon-capture and -storage of the produced $CO_2$.[75,76] Lastly, biomass can be used as a sustainable source of hydrogen, directly through gasification, or indirectly through anaerobic digestion or fermentation followed by steam reforming.[77]

**2.2.2. Ammonia synthesis loop.** New developments in the ammonia synthesis loop focus on two main aspects. The first focus is on modifying the Haber–Bosch process by decreasing the operating temperature and pressure, by using more active catalysts and highly efficient separation of ammonia with sorbents, which is coined the absorbent-enhanced Haber–Bosch process.[6,68] The second focus is on novel ammonia synthesis methods, such as electrochemical ammonia synthesis,[78,79] photochemical ammonia synthesis,[80,81] plasma-driven ammonia synthesis,[82–84] homogeneous ammonia synthesis,[66,85] and chemical looping approaches.[86,87] Novel ammonia synthesis methods were recently reviewed by various authors.[14,18,66,88] The current status of alternative ammonia synthesis methods is listed in Table 2.

*Modifying the Haber–Bosch process.* The first strategy towards ammonia production from nitrogen and hydrogen under milder conditions is the development of more active catalysts. Over the past five years, substantially more active Ru-based catalysts were developed,[44,45,98–100] which can lower the minimum reaction temperature from about 350 °C to 200–250 °C.[88] This is especially relevant for small-scale ammonia production, as the reaction heat in small-scale plants is usually not heat-integrated with the hydrogen production. Thus, operating under mild conditions decreases heat losses.

Even though milder temperatures can be achieved by using better catalysts, the condensation process is limited by the partial pressure of ammonia in the gas phase for separation at −20 °C to 30 °C.[6] This leads to a minimum feasible pressure of about 100 bar.[95] Operation at lower pressure is only feasible by using alternative methods for ammonia removal. A wide variety of sorbents have been researched, among which metal halides and zeolites are most promising.[101,102] These solid sorbents allow for complete ammonia removal from the reactor effluent under milder pressures of 10–30 bar and at temperatures close to the temperature of the ammonia synthesis reactor, which is coined the absorbent-enhanced Haber–Bosch process.[68,103,104] This may allow for operating the hydrogen

**Table 2** Comparison of alternative ammonia synthesis methods. The reported energy requirement refers to the best available technology (BAT) or the best reported value in literature. The potential energy requirement refers to the energy requirement of such a process if the technology is successfully improved, and additional separation steps are included. The theoretical minimum refers to the theoretical minimum energy consumption for the reaction based on thermodynamics (separation steps are not included). Estimates based on ref. 55, 65, 66 and 89–95

| | Energy requirement (GJ $t_{NH_3}^{-1}$) | | | |
|---|---|---|---|---|
| | Reported | Potential | Theoretical minimum | TRL |
| **Benchmark electrolysis-based Haber–Bosch process**[a] | **33** | **26** | **21.3** | **7–9** |
| **Electrolysis-based Haber–Bosch processes with** | | | | |
| Absorbent-enhanced synthesis loop | 47–50 | 30–35 | — | 4–5 |
| Non-thermal plasma technology with mild excitation | 155 | 50–65[b] | 22.3[c] | 1–3 |
| Non-thermal plasma technology, $N_2$ & $H_2$ dissociation in plasma | — | — | 87.4[c] | 1–3 |
| **Electrochemical & photochemical synthesis** | | | | |
| Electrochemical synthesis | 135 | 27–29 | 18.6 | 1–3 |
| Photochemical synthesis | — | 200 | — | 1–3 |
| **Other technologies** | | | | |
| Electro-thermochemical looping | 64 | — | 55 | 1–3 |
| Homogeneous catalysis | 900 | — | 159 | 1–3 |

[a] The energy requirement is for large-scale plants. Upon scale-down, the energy efficiency will be lower (see Fig. 4). [b] Electrolysis for hydrogen production, nitrogen production, plasma-catalysis and recycling of the synthesis gas are included in the consideration. The potential energy requirement is based on an energy consumption of about 35 GJ $t_{NH_3}^{-1}$ for $H_2$ production *via* low temperature electrolysis and $N_2$ purification. Plasma-activation of $N_2$ can lower the $N_2$ dissociation barrier by about 70 kJ $mol^{-1}$ over Ru catalysts.[96] We assume that this is the energy input of the plasma. This results in an energy consumption of 2.1 GJ $t_{NH_3}^{-1}$, the ammonia separation amounts to about 10 GJ $t_{NH_3}^{-1}$ with a metal halide or zeolite material. At ammonia outlet concentrations above 1 mol%, the recycle cost is negligible.[95] Additional details can be found in ref. 97. [c] The theoretical energy consumption is based on the heat of reaction for the formation of ammonia from $H_2O$ and $N_2$ *via* electrolysis of $H_2O$ to $H_2$ and $O_2$, with subsequent hydrogenation of $N_2$ with $H_2$. Furthermore, additional energy is required for mild excitation of $N_2$ by the plasma, which is assumed to be 2.1 GJ $t_{NH_3}^{-1}$ (see foornote *b*). This results in a total energy of 22.3 GJ $t_{NH_3}^{-1}$ for the mild excitation case. When $N_2$ and $H_2$ are fully dissociated in the plasma, this requires 66.1 GJ $t_{NH_3}^{-1}$. Combined with the 21.3 GJ $t_{NH_3}^{-1}$ required in the base case, this results in a total energy consumption of 87.4 GJ $t_{NH_3}^{-1}$ for the $N_2$ & dissociation in plasma case.

 

Table 3 Comparison of ammonia separation technologies. Based on ref. 6, 103 and 107–109

| | Condensation | Metal halides | Zeolites |
|---|---|---|---|
| Separation temperature (°C) | −20 to 30 | 150–250 | 20–100 |
| Desorption temperature (°C) | — | 350–400 | 200–250 |
| Pressure (bar) | 100–450 | 10–30 | 10–30 |
| Energy consumption (GJ $t_{NH_3}^{-1}$) | 3–5 | 6–11 | 8 |
| Ammonia at outlet (mol%) | 2–5 | 0.1–0.3 | 0.1–0.3 |
| Ammonia capacity (wt%) | 100 | 5–30 | 5–15 |
| Ammonia density (kg $m^{-3}$) | 680 | 100–600 | 30–90 |
| Chemical stability | - | Low/medium | High |
| TRL | 9 | 4–5 | 4–5 |

and nitrogen production at the same pressure as the ammonia synthesis loop.[6] Furthermore, ammonia may also be stored on the sorbents.[105,106] The conditions for various ammonia separation technologies are listed in Table 3.

*Novel ammonia synthesis methods.* In academia, research is being pursued into alternative methods for nitrogen fixation. The main research tracks involve electrochemical & photochemical ammonia synthesis,[78–81] plasma-driven ammonia synthesis,[82–84] homogeneous ammonia synthesis,[66,85] and chemical looping approaches.[86,87] Plasma-driven ammonia synthesis is discussed from section 3 onward and will not be discussed further in this section.

By far, most research has been conducted on electrochemical ammonia synthesis.[78,79,110–112] This is due to the promise of reducing nitrogen directly from water and air (eqn (4)–(6)). Electrochemical ammonia synthesis only requires a relatively simple electrolysis setup, and both reactants can be generated in the same cell as the two opposing half-reactions.[112] However, electrochemical ammonia synthesis remains an unsolved scientific challenge,[112] due to the formation of hydrogen at lower overpotentials than ammonia over transition metals (see Fig. 5).[113,114] Electrochemical ammonia synthesis suffers from the high bond strength of the dinitrogen molecule (941 kJ $mol^{-1}$), as well as the large difference between the HOMO and LUMO in the molecule (1044 kJ $mol^{-1}$),[115] meaning that dissociation on the electrode surface is difficult. Furthermore, the solubility of nitrogen in aqueous electrolytes is limited, further favouring the formation of $H_2$ rather than ammonia.[14] The reported activities are so low, that ammonia impurities in the surroundings sometimes lead to false positives.[116,117] Current strategies include the use of three-dimensional materials and bio-inspired materials, as well as the use of non-aqueous electrolytes.[92,118,119]

$$H_2O \rightarrow 2H^+ + \frac{1}{2}\,O_2 + 2e^- \quad (4)$$

$$H_2 \rightarrow 2H^+ + 2e^- \quad (5)$$

$$N_2 + 6H^+ + 6e^- \rightarrow 2NH_3 \quad (6)$$

Photochemical ammonia synthesis has also gained interest in recent years, due to the potential simplicity of directly converting photons *via* electrochemical activation of $N_2$ and $H_2O$ to ammonia.[80] However, photochemical ammonia synthesis suffers from similar challenges as electrochemical ammonia synthesis, with the additional difficulty of supplying electrons by light.[120] So far, research on photocatalytic ammonia synthesis has not yielded any promising results.[81]

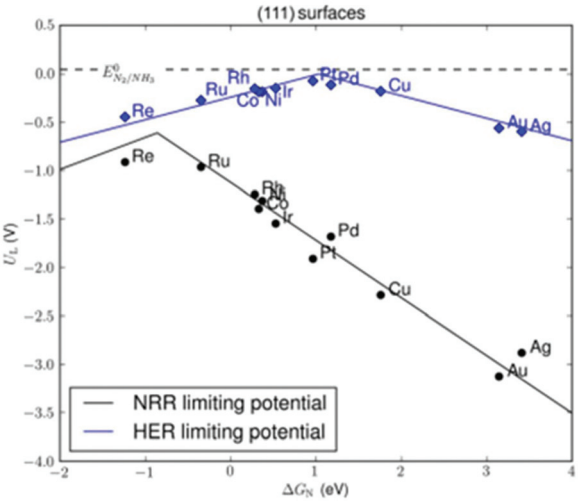


Fig. 5 Limiting potential for the nitrogen reduction reaction (NRR) and hydrogen evolution reaction (HER) over different transitions metals. Reproduced from ref. 113.

Research has been conducted on homogeneously catalysed ammonia synthesis, which is mostly aimed at understanding and intensifying nitrogenase (the nitrogen fixation method of plants).[66,85] The potential for practical application is limited for homogeneously catalysed ammonia synthesis (see Table 2). However, nitrogenase-like complexes may find applications for on-site fertilizer production on the seeds of plants.[121]

Chemical looping approaches have also been researched,[86,87] inspired by the industrial Frank–Caro process in the early 20th century.[18,19] Sometimes chemical looping approaches are used in electrochemical systems.[122] By separating the nitrogen reduction, hydrogen oxidation and ammonia synthesis steps, it is possible to operate the individual steps at the optimal conditions to boost conversion and selectivity to ammonia. The main drawback is that every step occurs at different conditions, implying temperature sweeps within a cycle. Switching between these conditions decreases the energy efficiency of the full process.

## 3. Plasma catalysis

As discussed in section 2, decarbonizing and decentralizing ammonia synthesis requires novel methods for the conversion of nitrogen and hydrogen. Although electrochemical (and to a lesser degree photochemical) ammonia synthesis have received substantial attention in recent years, this remains a scientific challenge. Plasma activation of the stable $N_2$ molecule is another alternative for electron-driven ammonia synthesis,[83,123–126] inspired by the Birkeland–Eyde process of

the early 20th century.[17,18] Next to nitrogen fixation, plasma-driven conversion has attracted recent attention for $CO_2$ conversion and methane coupling.[83,125,127] In the current section, plasma technology is introduced, with a focus on nitrogen fixation to ammonia. Afterwards, reported activities, mechanisms and prospects for plasma-driven ammonia synthesis are discussed in sections 4–6.

### 3.1. Plasma properties

Plasma can be considered as the fourth state of matter, in which electrons, various types of ions, molecules and their derived radicals and excited species show collective behaviour, which is strongly determined by the influence of electrodynamics due to the charged particles.[82,83,123] This state of matter is typically reached by adding energy to a gas. However, the transition is far more complex than the transitions between solids, liquids and gases.

Plasmas exist in a large variety. The type of plasmas used in plasma catalysis operate near room temperature up to several thousand K, and are typically partially ionized with ionization degrees of $10^{-4}$ to $10^{-6}$. The latter type of plasmas find many industrial applications, *e.g.* in microelectronics, coating deposition and lighting, as well as emerging applications in green chemistry, pollution control, gas conversion and medical applications.[128]

One important parameter identifying a plasma, certainly for applications of plasma catalysis as discussed in this review, is the so-called reduced electric field ($E/N$), *i.e.*, the electric field strength ($E$, in V m$^{-1}$) over the total gas number density ($N$, in m$^{-3}$). $E/N$ is mostly expressed in Townsend (Td), where 1 Td corresponds to $10^{-21}$ V m$^2$. The reduced electric field determines the electron energy distribution function (EEDF), which gives the likelihood of finding an electron with a certain energy in the plasma.

Partially ionized plasmas, generated from a gas breakdown upon application of an electric field, are classified as non-thermal plasmas, because only the electron temperature is elevated far above room temperature. Furthermore, the gas molecules in the plasma can be rotationally, vibrationally or electronically excited, and the degree of excitation can be expressed by rotational, vibrational and electronic excitation temperatures. The electronic excitation temperature is typically comparable to the electron temperature, while the gas (translational) temperature, ion temperature and rotational temperature are also typically equal to each other. The vibrational temperature, however, can be elevated in a plasma above the gas temperature, *i.e.*, when the vibrational levels are overpopulated compared to a Boltzmann distribution at the gas temperature. It is this concept which is often exploited in gas conversion applications to increase process efficiencies and yields.[83,129,130]

The various electron impact processes occurring in the plasma, and their corresponding rates, depend on the EEDF and the electron density, which in turn depend on the reduced electric field in the plasma. Next to rotational, vibrational and electronic excitation, ionization and dissociation of the gas molecules can occur as well. In Fig. 6, we plot the fraction of electron energy lost to those various processes in an $N_2/H_2$ (25/75%) gas mixture, as a function of the reduced electric field (bottom $x$-axis) and mean electron energy (top $x$-axis). Based on the electron impact collisions with $N_2$ (Fig. 6(a)), we can identify three different plasma regimes:

- Regime I: Below 20 Td, where vibrational excitation of $N_2$ is dominant.
- Regime II: Between 20 and 200 Td, where electronic excitation of $N_2$ is most significant.
- Regime III: Above 200 Td, where ionization (mainly from $N_2$ ground state to $N_2^+$) and dissociation are the most important $N_2$ electron impact processes.

Note that this figure specifically applies to this gas mixture, and to a fixed gas temperature of 400 K and vibrational temperature of 3000 K; other assumptions lead to somewhat different borders between the different regimes, so they only give an indication, but are no hard numbers.

For the sake of information, we plot in Fig. 6(b) the same processes for $H_2$. Note that vibrational excitation of $H_2$ has a contribution less than 0.1%, in spite of its higher fraction in the gas mixture. On the other hand, electronic excitation and dissociation of $H_2$ start to be important from much lower $E/N$ values, because the $H_2$ bond dissociation energy is much lower than for $N_2$.

### 3.2. Feedstocks

Various feedstocks have been used for plasma-driven ammonia synthesis, but most research focuses on $H_2$ and $N_2$ as feedstocks. Furthermore, various authors researched plasma-driven ammonia synthesis from $CH_4$ and $N_2$ (*e.g.*, the feedstock for the SMR-based Haber–Bosch process),[133–136] as well as $H_2O$ and $N_2$ (*e.g.*, the feedstock for the electrolysis-based Haber–Bosch process).[137–142] The challenge with using $CH_4$, and even more with using $H_2O$, is that the ammonia synthesis becomes endergonic. Although such a reaction can be driven by plasma, the energetically favourable reverse reaction is likely to compromise efficiency.

On the other hand, plasma technology may be a pathway to provide the energy required to form ammonia from $H_2O$ and $N_2$, as the reaction is highly endothermic. Furthermore, $H_2O$ is a sustainable $H_2$ source. However, a drawback of using $H_2O$ and $CH_4$ as a hydrogen source is the presence of carbon or oxygen, implying that ammonia is not the only product of the reaction. In the case of $CH_4$ and $N_2$ as reactants, C≡N-compounds such as hydrogen cyanide (HCN) are potentially formed, which are extremely poisonous and flammable. For the $H_2O$ and $N_2$ as feedstock, other reaction products include $NO_2^-$, $NO_3^-$, and $NH_4^+$ in the aqueous phase and $H_2O_2$, $NO_x$, $O_3$ and $H_2$ in the gas phase.[137,138] The lowest energy consumption reported for $NH_3$ from $H_2O$ and $N_2$ is about 5600 GJ t-$NH_3^{-1}$.[137] As follows from electrochemical ammonia synthesis, finding a catalyst selective for ammonia synthesis as compared to $H_2$ production is an unsolved scientific challenge.[116]

 

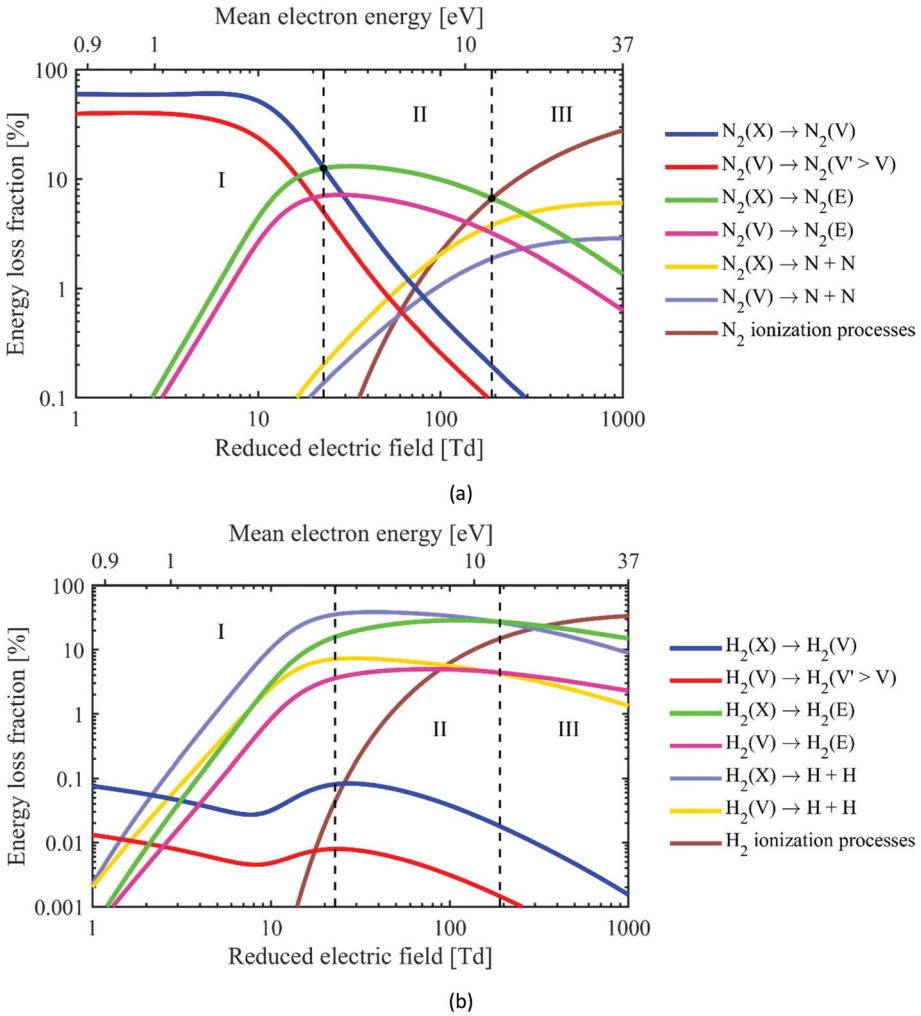


**Fig. 6** Fraction of electron energy transferred to various important electron impact collisions (*i.e.* vibrational excitation, electronic excitation, dissociation and ionization) in an $N_2/H_2$ 25/75% mixture at 400 K and a vibrational temperature of 3000 K,[131,132] as a function of the reduced electric field (bottom *x*-axis) and the corresponding mean electron energy (top *x*-axis), both for $N_2$ (a) and $H_2$ (b). Note the different *y*-axis between (a) and (b). The notations (X), (V) and (E) denote the ground state, vibrational levels and electronically excited levels of the molecules, respectively.

### 3.3. Plasma reactors

Throughout the years, different kinds of plasmas have been studied for the plasma-catalytic synthesis of ammonia from $N_2/H_2$ feedstocks. In addition, $N_2/H_2O$ non-catalytic plasma–liquid systems have recently been investigated for ammonia synthesis. In Fig. 7 we depict the accumulation of approximate number of publications on the various plasma sources through time.

A general consideration for the material choice of the plasma reactor is the corrosive nature of ammonia. Thus, carbon–steel and Cu-containing alloys should not be used. Stainless steel equipment is used for industrial ammonia synthesis, at partial ammonia pressures of up to 75 bar. In case of plasma-catalysis, partial ammonia pressures are substantially lower (typically in the order 0.01 bar). Thus, corrosion due to ammonia should not be a critical issue in plasma reactors.

Glow discharges (GDs; in direct current (DC) mode) are the simplest form of self-sustained gas discharges. They are created between two electrodes, *i.e.* a cathode and anode, to which a constant high potential difference is applied. Electrons are emitted from the cathode and accelerated towards the anode, causing collisions with the gas in the discharge tube. Electron impact excitation creates excited species, which emit photons upon decay to lower levels. This explains the name of these "glow" discharges. Electron impact ionization creates ions and new electrons. The combination of electron emission at the cathode and ionization in the bulk of the gas makes the discharge self-sustained. Such glow discharges are characterised by a well-defined plasma structure and the emission of light, *i.e.* a glow, at specific locations of the discharge. GDs can be created at low pressure, but also at atmospheric pressure.

Radio-frequency (RF) plasmas, typically operating at low pressure, can exist in capacitively coupled (CC) or inductively coupled plasma (ICP) mode. CC RF plasmas are in their simplest form also created by applying a potential difference

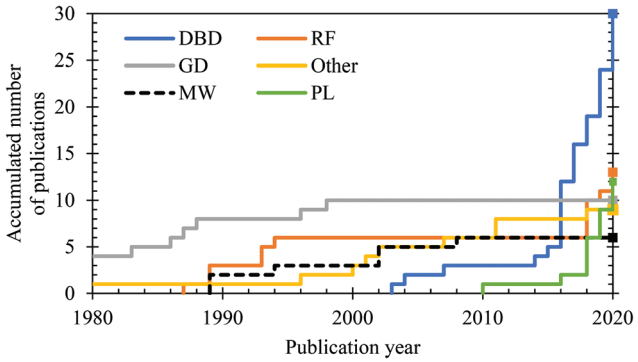


**Fig. 7** Approximate accumulated number of publications on ammonia formation from $N_2/H_2$ in the various plasma reactors studied throughout time, as well as from $N_2/H_2O$ non-catalytic plasma–liquid systems. The listed plasma reactors are dielectric barrier discharge (DBD),[96,131,142,143–149,150–159,160–169] (low pressure) glow discharge (GD),[170,171,172–179,180] microwave plasma (MW),[181–186] (low pressure) radio frequency discharges (RF),[181–183,187–193,194–196] miscellaneous plasma reactors and devices (other),[197–204] and plasma–liquid systems (PL).[87,137,138–140,205–209,210,211]

between two electrodes, just like in low pressure GDs. The important difference is that the potential difference is not constant (direct current, DC), but alternating current (AC), with a frequency in the RF range (typically 13.56 MHz). In ICP RF plasmas, an electric current flows through a coil, which can be wound over the plasma reactor or placed on top of it, and it induces an RF electric field in the plasma. The ions only experience a time-averaged electric field, as their characteristic plasma frequency is typically lower than the applied RF frequency, while the light electrons can follow the fluctuating electric field, so they can be more accelerated, giving rise to more electron impact (electronic) excitation, ionization and dissociation of the gas molecules. Vibrational excitation is less important, because of high values of the reduced electric field.

Microwave (MW) discharges are another type of high frequency discharge, typically operating in the GHz regime. In contrast to GDs and CC RF discharges, the plasma reactor is electrode-less, and the power to break down the gas is delivered by the microwaves. Most common is a setup where the microwaves are transferred with waveguides to a quartz discharge tube through which the gas flows, but also other MW-based plasma setups are possible.[212,213] MW discharges can operate from low pressure[212] to atmospheric pressure.[213] Upon increasing the operational pressure, the plasma becomes increasingly more thermal.

A dielectric barrier discharge (DBD) consists of two opposing electrodes with at least one electrode covered by a dielectric material (*e.g.*, quartz or alumina). An alternating voltage is applied on the electrodes. Common voltage amplitudes are in the order of a few kV and the frequency is typically in, but not limited to, the kHz range.

DBDs for gas conversion applications operate in the filamentary regime with strong, temporally and spatially isolated small discharges throughout the gaseous discharge gap. The complexity of this filamentary behaviour leads to confusing nomenclature in literature. Section 3.4 provides an overview of the most common terms and the types of discharges that are observed in (packed) DBDs. In recent years, most plasma-based ammonia synthesis is performed in DBD reactors (see Fig. 7), because they operate at atmospheric pressure, they are very flexible and easily allow the integration of catalysts.

Besides plasma-catalytic ammonia synthesis, carried out in the above-described gas-phase plasma reactors, ammonia synthesis has recently also been realized in plasma–liquid systems, without using catalysts. This is usually accomplished by plasma jets, as typically used for plasma medicine applications.[214] A plasma jet can operate in argon or helium, but also directly in air or $N_2$ gas. The plasma is created inside a tube, consisting of (usually) two electrodes, through which the gas flows. Many different designs and geometries are possible, *e.g.*, the powered electrode can be a ring-shape, needle, *etc*. The counter-electrode can be a ring, but the target to be treated (*e.g.*, liquid in this case) can also act as counter-electrode. Due to the gas flow, the plasma can exit through a nozzle, creating an effluent, or jet. The jet comes into contact with the ambient atmosphere, causing the creation of various reactive oxygen and nitrogen species, or with a more controlled environment, *e.g.* pure $N_2$, which is more interesting for ammonia synthesis. Due to the gas flow, the plasma effluent can reach the liquid, located at a distance of several mm from the tip of the plasma device, and the reactive plasma species can be transferred to the liquid phase. The reactive plasma species react with $H_2O$ molecule forming ammonia, but also $NO_3^-$ and $NO_2^-$, among others, limiting the selectivity of the ammonia synthesis.

### 3.4. Discharge types

As mentioned above, DBDs relevant for plasma catalysis (and gas conversion applications in general) operate in the filamentary regime. The plasma exhibits small discharges, or *micro-discharges*, that do not encompass the complete discharge reactor, and which are often called *filaments*, *i.e.* thin conducting wires. Sometimes they are also called *streamers*. However, streamer discharges are not specific to occur in DBD systems alone.[215,216] Wang *et al.* also described a micro-discharge between two packing beads as a *local discharge*,[217] while Kim *et al.* used the term *partial discharges*[218–221] after Mizuno *et al.*,[222] and Butterworth *et al.* used the term *point-to-point discharges*.[223]

*Surface streamers*, *surface discharges* or *surface ionization waves* are terms used for micro-discharges that are observed after a streamer or filament reaches a surface, such as a packing bead. Once the micro-discharge reaches the surface, the discharge continues in a lateral expansion across the surface. This lateral expansion is facilitated by strong electric fields and the ionization processes taking place in the growth direction of the discharge.[224,225]

An *afterglow* normally describes the effluent of a plasma reactor. However, the term is sometimes used more broadly to indicate that (plasma) species are no longer exposed to

 

plasma conditions corresponding to micro-discharges. Liu *et al.* described those two usages as a spatial and temporal definition, respectively.[226]

*Homogeneous plasma* or *uniform plasma* are terms that have been seen in relation to the filamentary regime of DBDs. This can be confusing because a DBD can operate in either a homogenous or in a filamentary regime. Still, the filamentary plasmas have been described as becoming more uniform, or more homogeneous when a packing is introduced.[156] In addition, such a description has been used when the micro-discharges are still present, but of lower importance.[163]

*Partial surface discharging*, as used by Peeters *et al.*[227] refers to the fact that not the whole surface area of the electrodes in a DBD reactor has to actively contribute to the discharge. This is due to the charge deposited on the electrode or dielectric surfaces being non-uniform or spatially isolated, due to the overall discharge consisting of small micro-discharges. This influences some electrical characteristics of the DBD.[227] This effect is generally important in packed bed DBDs due to the obstructions in the plasma.

### 3.5. Coupling of plasma and catalyst

Coupling plasma and catalysis is complex. Previously, such mutual influences of the plasma and the catalyst were extensively discussed by Neyts *et al.*[125,228,229] and Kim *et al.*[219] Recent modelling investigations and characterization have provided novel insights.[230,231] This subsection sets the stage for the assessment of plasma-catalytic ammonia synthesis.

Plasma-catalytic reactors are classified as in-plasma catalysis reactors or post-plasma catalysis reactors.[90,219] In case of in-plasma catalytic reactors, also termed plasma-driven catalytic reactors, the plasma and the catalyst are located in the same position in the reactor.[219] In case of post-plasma catalytic reactors, also termed plasma-assisted catalytic reactors, the plasma generation and the catalyst bed are separated in space.[219] While in-plasma catalysis can be used to activate short-lived plasma-activated species over a catalyst, post-plasma catalysis is only relevant for long-lived species.[219] Thus, plasma catalysis can benefit from the mutual influence of the plasma and the catalyst on one another.

**3.5.1. Synergy and mutual influence.** Plasma catalysis sometimes leads to synergistic effects, in which the result of combining the plasma and the catalyst is larger than the sum of the individual contributions of the plasma and the catalyst.[232] Synergy may be defined in terms of conversion, reaction rate or selectivity. It should be noted that in the case of ammonia synthesis, selectivity is not relevant because there are no by-products. However, plasma-catalyst interactions and synergies thereof are not trivial to uncover, as the underlying principles of plasma catalysis are not fully understood.[231,233,234] Various possible plasma-catalyst interactions have been proposed for ammonia synthesis, as shown in Fig. 8.

A multidisciplinary approach is required to understand the mutual influence of the plasma and the catalyst,[219] covering various time-scales and length-scales.[90,231,235,236] So far, most information is obtained by macroscopic performance testing of plasma catalysis reactors. Van Durme *et al.*[237] were the first to systematically categorize the mutual influence of a plasma and a catalyst, a topic heavily discussed thereafter.[125,219,228,229,231,233,234] Possible mutual influences of a plasma and a catalyst have been reviewed by Kim *et al.*,[219] Neyts *et al.*[125,228,229] and Whitehead.[231,233,234] The complexity is even more severe, as any change in the catalyst will induce changes in the plasma, which again influence the catalyst. Thus, effects in plasma-catalytic interactions can generally not be isolated.[233,238]

The various species present in the plasma environment include electrons, positive and negative ions, photons, radicals, and neutral atoms and molecules in ground state or excited in vibrational or electronic modes.[90] These species may interact with the catalyst in various manners, and catalyst may influence the conversion of $N_2$ and/or $H_2$ in the presence of a plasma in three manners, namely (1) by modifying the plasma characteristics, (2) by exploiting the radicals from the plasma environment for reaction pathways other than simple recombination, or (3) *via* surface reactions of plasma-activated species on the catalyst surface.

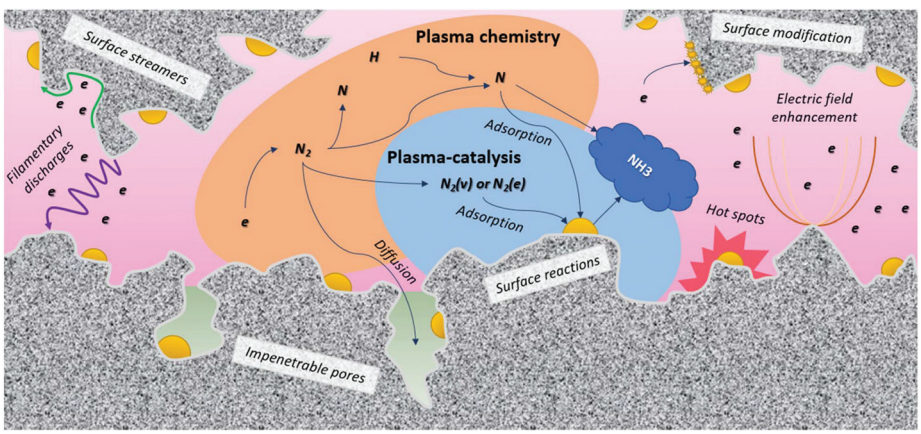


Fig. 8 Plasma-catalyst interactions. Inspired by ref. 228.

The first mechanism, *i.e.* modifying the plasma characteristics, may influence the plasma chemistry far from the surface, when the catalyst is applied on dielectric packing material. A commonly encountered effect is the electric field enhancement and consequently a decreased plasma onset voltage, as was substantiated by simulations.[230,239–241] The electric field enhancement will also enhance the electron temperature,[230,239–241] which may shift the importance of various electron impact reactions, and thus affect the plasma chemistry. In addition, micro-discharges may form on the surface of the catalytic packing, or even the discharge may entirely move from the gas phase to the catalyst surface, depending on the dielectric constant of the packing beads.[217,234]

The second mechanism, *i.e.* exploiting the plasma radicals for reactions other than recombination, proceeds *via* facile adsorption on catalyst surfaces,[90] without any barrier. In case of noble metals, all further reactions proceeding on the catalyst surface are downhill and the surface has either limited or no activating effect on the hydrogenation reactions. On the other hand, surface reactions can have a strong effect on the dominant reaction pathways and thus on the product distribution. This can even lead to increased conversion when the surface indeed favours reaction pathways to products over recombination reactions, forming back the reactants. The production of radicals and ions may also open alternative surface reaction pathways,[228,242] that are not accessible in thermal catalysis. It should also be noted that radicals and ions in the plasma may react on the surface with other surface species which are formed *via* dissociative adsorption of non-activated molecules. This mechanism is discussed in more detail in section 5.2.

The third mechanism, *i.e.* surface reactions of plasma-activated species, is complex and often not well understood. Dissociative chemisorption can be enhanced *via* vibrational or electronic excitation of a molecule,[123,243] decreasing the apparent activation barrier and increasing the reaction rate in case the dissociative adsorption step is rate limiting in thermal catalysis.[96,244] A recent study also showed that vibrational excitation could enhance Eley–Rideal reactions of molecular species.[245] Such reactions are typically negligible under thermal conditions and it is not fully understood to what extent they contribute to the total conversion under plasma conditions. These mechanisms and how they impact the total conversion and energy efficiency will be discussed in more detail in section 5.3.

Besides effects from the presence of reactive plasma species, the surface properties of the catalyst such as the work function and consequently the activity of the surface might be altered due to the presence of plasma, *e.g.*, by the electric fields or surface charging.[246–248] Physical modifications of the catalyst surface may also occur due to bombardment with energetic plasma species, causing reduction of the catalyst, coke formation, changes in the physicochemical properties of the catalyst (such as the catalyst work function), and the formation of hot spots. Furthermore, it was reported that surface cracking and peeling of metal nanoparticles can occur in DBD reactors.[249] Similarly, changes in the surface morphology of a metal oxide catalyst after plasma treatment were reported after plasma-illumination in a DBD reactor.[250]

A pre-requisite for effective interaction between the plasma and the catalyst is that the plasma-activated species reach the catalytic surface before recombining or decaying to the ground state molecules.[234] Plasma-activated species have a limited lifetime, and thus a limited traveling distance by diffusion, before recombining into neutral molecules, or decaying to the ground state.[219] A direct interaction between the plasma and the catalyst surface is attained when the distance between the plasma and the catalyst surface is smaller than the maximum traveling distance of plasma-activated species.[219] This is especially relevant when the catalyst is porous, as shown in Fig. 8. Large pores allow the generation of plasma inside the pores, but this is only possible for pores in the (sub-)micron range.[230,251–253] Indeed, a prerequisite is that the pore size must be larger than the Debye length, which is defined by the electron density and temperature in the plasma. In helium, characterized by homogenous plasma, computer simulations revealed that plasma can only be formed in pores with diameters typically above 10 μm.[252,254,255] On the other hand, molecular plasmas typically exhibit streamers, with higher electron density and smaller Debye length. Hence, computer modelling predicts that plasma streamers can propagate in pores of several 100 nm diameter, depending *e.g.*, on the applied voltage.[253,256] It should be noted that the majority of the pores in a typical support material are smaller than 50 nm. Therefore, only plasma-activated species with a sufficiently long lifetime can penetrate into the pores, while most other species recombine or decay to the ground state before reaching the active catalyst surface within the pores. Thus, the contribution of the external surface area is likely to dominate in most cases.

**3.5.2. Catalyst selection considerations.** Depending on the plasma conditions and the chosen catalyst material, different plasma-activated species can determine the catalytic reactions (see Fig. 6). In order to optimize the plasma-catalyst synergy, it is crucial to couple the right catalyst to the right plasma.

In plasmas with a low degree of dissociation and a high degree of excitation (vibrational or electronic), plasma-activation is used to decrease the operating temperature for processes that are limited by dissociative adsorption. Typically, the optimal active metal is a more noble metal than the optimum for thermal catalysis, which desorbs reaction products easily and thus the operating temperature can be low. Dissociative adsorption of reactants is usually limiting the reaction rate for noble metals. Part of the activation barrier of dissociative adsorption may be overcome through vibrational or electronic excitation of molecules, explaining the plasma-enhanced catalytic activity over a noble metal. The catalyst still has an activating role in this case, as $N_2$ is not fully dissociated in the plasma environment. Apart from metallic catalysts, metal nitrides have also been reported for ammonia synthesis.[47,257] Plasma-activation of metals with nitrogen plasmas may yield metal nitride catalysts.[258] Hargreaves[46]

 

recently reviewed metal nitride catalysts active for ammonia synthesis.

In plasmas with a higher degree of dissociation, the ideal catalysts will usually be very different from those used in thermal catalysis. Plasma-generated radicals do not need to be dissociated over a surface, as dissociation already occurs in the plasma. Thus, the surface influences recombination reactions, as well as consecutive reactions with *e.g.* H atoms on the catalyst surface. Plasma activation of reactants *via* formation of radicals often opens pathways that are thermodynamically impossible for ground state reactants; in that case the use of traditional catalysts is likely to be counterproductive as these will catalyse the reverse reaction, back to reactants. Several materials may enhance reaction pathways, such as consecutive reactions with H atoms forming ammonia, instead of recombination of radicals to $N_2$. Transition metals may be used to hydrogenate the adsorbed $NH_x$ ($x$ = 0–2) radicals. For these catalysts, efficient plasma-activation of reactants towards radicals is required.[259] Therefore, the choice of the catalyst is less determined by chemical properties and more by properties influencing the discharge characteristics (*e.g.* dielectric properties and morphology), thereby influencing the plasma-phase dissociation of activated molecules. A method to modify the plasma by radicals was proposed by Akay *et al.*,[152,168,260] who used a mix of a dielectric material with a supported transition metal catalyst in the plasma reactor. The dielectric material acts as a plasma catalyst promoter (PCP), which modifies the plasma characteristics, whereas the transition metal catalyst performs the catalytic function.

Apart from the choice of the active metal, the choice of the support and promoter composition affect the activity in some cases.[96] As plasmas can only be generated in (sub)-micron pores (*cf.* previous section), oxides with highly porous structures with pore sizes below 1 μm and large internal surface areas are not beneficial for maximum interaction between the active metal catalyst and the plasma (see Fig. 8).[230] This is very different form thermal catalysis, requiring an as high as possible active surface area and therefore support materials with high surface area, in order to maximize the productivity per unit of volume of chemical reactors.

# 4. Assessment of plasma-driven ammonia synthesis

This section provides an overview of the most significant developments in plasma-driven ammonia synthesis, with a focus on the coupling between fundamentals from heterogeneous catalysis and plasma catalysis. This forms a framework for plasma-driven ammonia synthesis, and the mechanisms involved. Extensive historical accounts can be found in other reviews.[82,84,90,141,261] The aim of this section is to show how recent insights in mechanisms can aid in the development of the field. The energy efficiency and conversion for various plasma reactor types are compared, describing the state of the art. The discussion on the mechanisms and catalyst selection is coupled with the energy efficiency.

## 4.1. Performance in various types of plasma reactors

Plasma-driven ammonia synthesis was first independently reported by Morren and Perrot in a DBD reactor in 1859,[262] two years after the first report of plasma-driven conversions with a DBD reactor by Werner von Siemens.[263] In the late 19th century, various authors attempted plasma-driven ammonia synthesis, among whom Berthelot.[262] Furthermore, ammonia was first synthesized in a glow discharge by Donkin in 1973.[264] In general, however, plasma-driven ammonia synthesis was sporadically researched until the 1980s.[262,265,266] Between 1980 and 2000, low pressure glow discharges (LPGDs) received a lot of attention.[170,171,173–180,181–183,267–272] In these publications, the surface (both catalytic and non-catalytic) was often related to the ammonia formation. Ions, more specifically $N_2^+$ and $N_2H^+$, were often mentioned to play an important role in the formation of ammonia. Nowadays, atmospheric pressure DBDs are studied most, although some papers also describe low pressure MW and RF discharges.[181–183,187,190–192,194–196]

A summary of quantified plasma-driven conversions to ammonia in various plasma reactors under a wide variety of conditions is shown in Fig. 9. An energy yield of 100–200 g-$NH_3$ kW $h^{-1}$ is required to be competitive with alternative technologies for small-scale ammonia synthesis.[90] Furthermore, an ammonia concentration of about 1.0 mol% (10 000 ppm) is required to minimize the energy cost of separation and recycling in case of an atmospheric synthesis loop,[95] as an ammonia partial pressure of 0.01 bar is required for effective ammonia removal in solid sorbents.[103,273–275] Therefore, low pressure plasma reactors such as MW and RF plasmas require a near complete conversion at an energy yield of 100–200 g-$NH_3$ kW $h^{-1}$, because separation of ammonia is not feasible. The highest energy yield reported so far is

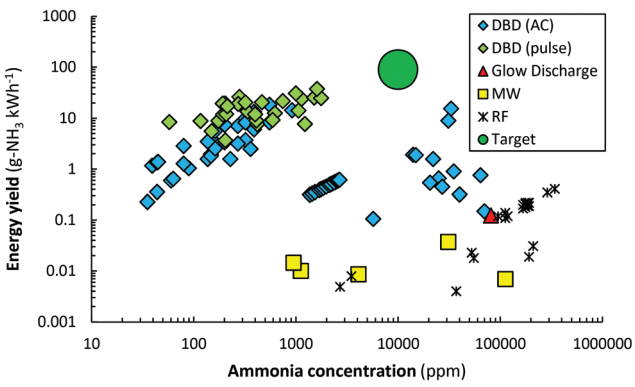


**Fig. 9** Reported energy yield *vs.* ammonia concentration. Constructed and extended from ref. 96. Original references: DBD (AC),[144,146–148,151–153,159,164–166,169,276,277] DBD (pulse),[158,165] Glow Discharge,[174] MW[186,278,279] and RF.[182,187,188,190–192,194] In some cases, the reported units have been converted to g-$NH_3$ kW $h^{-1}$ for the energy yield, and ppm for the ammonia concentration. We refer the reader to the recent review of Carreon[261] for the reported energy efficiency for specific metals.

37.9 g-$NH_3$ kW $h^{-1}$.[165] Hereafter, plasma reactors for ammonia synthesis from $H_2$ and $N_2$ are discussed.

**4.1.1. DBD reactors.** Most literature is available on plasma-driven ammonia synthesis in a DBD reactor. Already in 1859, Morren and Perrot reported experiments with a DBD reactor.[262] Modern attempts at plasma-driven ammonia synthesis in DBD reactors date from the 1950s, 1960s and beyond.[265,266] Especially since 2000, research on plasma-catalytic ammonia synthesis is mostly performed in DBD reactors.[82,84,261] Various reactor configurations without and with packed bed have been attempted. An overview of the energy yield *vs.* ammonia concentration for various packing materials is shown in Fig. 10.

*Electrode materials.* Various authors have researched either ammonia synthesis, or ammonia decomposition, with various electrode materials.[150,153,174,266,280] Iwamoto *et al.*[153] attributed a trend in ammonia synthesis rate for wool-like electrodes to the binding strength of $N_{ads}$ on the metal surface. On the other hand, Yin *et al.*[174] reported that the ammonia yield increases with increasing electron work function of the electrode material. An increased electron work function implies that the electrons released upon discharging have a higher energy, making dissociation of $N_2$ in the gas phase more likely.

*Oxides.* A drawback of a DBD reactor without a packing is the high ratio between plasma volume and surface area for catalytic reactions. Therefore, most authors introduced packing materials, such as oxides,[143,146,155,161,162,167,199,281] dielectric materials,[146,149,161,166] and ferro-electrics.[147] Introducing a packing material can lower the discharge power required to ignite the plasma. Furthermore, the presence of a packing material can alter the plasma discharge characteristics.[149,161] Surface functionalization of the oxide can also alter the plasma discharge characteristics.[149] The capacitive and discharge regimes can be modified by the dielectric constant of the material.[161]

*Ru-Catalysts.* The presence of supported metal particles may introduce hydrogenation sites for atomic nitrogen and/or molecular $N_2$. Ru-Catalysts have been studied most among supported metal catalysts.[90,96,131,144,145,148,151,159,160,165,169,282]

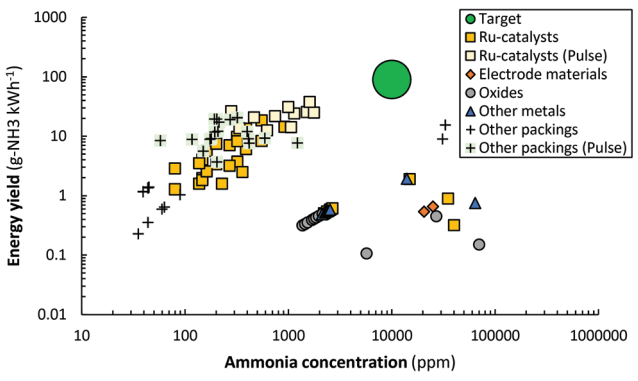


Fig. 10 Reported energy yield *vs.* ammonia concentration for DBD reactors (AC and Pulse). Constructed and extended from ref. 96. Original references: DBD (AC),[144,146–148,151–153,159,164–166,169,276,277] DBD (pulse).[158,165]

Ru-Catalysts are known to have a high activity for ammonia synthesis under mild conditions.[41,283] The rate-limiting step for thermos-catalytic ammonia synthesis over Ru-catalysts is usually the dissociation of $N_2$.[41] Ru-Catalysts were first used in a membrane-like DBD reactor by Mizushima *et al.*[144,145] Afterwards, various authors attempted to disentangle the complexity of reactions in plasma-driven ammonia synthesis in a DBD reactor packed with Ru-catalysts.[90,96,148,151,159,160,165,169,282]

In order to distinguish between the rate of homogenous plasma-chemical ammonia synthesis, and the rate of heterogeneous plasma-catalytic ammonia synthesis over the Ru-catalyst, it is important that the rate in a DBD reactor packed with the bare support is low. For this reason, various authors reported conversions for the bare support, as well as the supported Ru-catalysts (sometimes with promoters).[148,151,282] Furthermore, various authors reported that the ammonia synthesis rate depends on the temperature.[90,96,165,282] Catalytic hydrogenation of nitrogen is possible only at sufficient high temperature, allowing for ammonia desorption. Below this onset temperature, plasma-driven ammonia synthesis must be attributed to plasma chemistry rather than catalysis.[282]

Various authors introduced alkali promoters,[96,148,151,165] which are known to enhance $N_2$ dissociation by lowering the $N_2$ dissociation barrier, as well as to enhance ammonia desorption for thermal-catalytic ammonia synthesis.[40,41,284–286] The highest reported energy yield for such a system is 37.9 g-$NH_3$ kW $h^{-1}$,[165] which is overall the highest reported energy yield to date (see Fig. 10). In case of plasma catalysis with molecular plasma-activated $N_2$, promoters can enhance the $N_2$ dissociation rate and thereby the ammonia synthesis rate.[96] However, in case the reaction proceeds *via* adsorption of $NH_x$ ($x$ = 0–2) radicals, the introduction of alkali promoters does not influence the conversion, apart from less desorption limitation of ammonia in the low temperature regime.[282]

*Other metal catalysts.* Next to Ru-catalysts, other supported metal catalysts were tested for plasma-catalytic ammonia synthesis (and ammonia decomposition).[131,152,156,157,159,168,276,277,279,280,287–292] In most cases, supported Co, Ni, and Rh catalysts are found to be most active among the tested catalysts.[131,156,159,276,277] Such metals have less ammonia desorption limitations than the classical Fe and Ru catalysts for thermal-catalytic ammonia synthesis. Mehta *et al.*[131,293] proposed that plasma-activation of $N_2$ *via* vibrational excitation leads to a lower barrier for $N_2$ dissociation, resulting in an enhancement for late-transition metals which are typically rate-limited by $N_2$ dissociation. On the other hand, Wang *et al.*[156] proposed that the introduction of metal nanoparticles on $\gamma$-$Al_2O_3$ changes the acid site strength, and thereby the ammonia synthesis rate on $\gamma$-$Al_2O_3$ acid sites. Herrera *et al.*[157] reported that the introduction of metal nanoparticles on $\gamma$-$Al_2O_3$ has a statistically insignificant difference in macroscopic discharge characteristics in the charge voltage characteristics compared to bare $\gamma$-$Al_2O_3$. Akay *et al.*[152,168] reported increased ammonia yield on introduction of dielectric materials in a physical mixture with supported Co and Ni catalysts, altering the plasma discharge characteristics.

 

*Other packings.* Solid sorbents have also been used for plasma-driven ammonia synthesis.[158,164] The ammonia is removed *in situ*, lowering the ammonia content in the plasma zone, thereby increasing the chance of activating the $H_2$ and $N_2$ reactants rather than the ammonia product. Metal halides, such as $MgCl_2$, can absorb ammonia in a solid solution, forming $Mg(NH_3)_xCl_2$.[294] Peng *et al.*[158] reported an energy yield of 20.5 g-$NH_3$ kW $h^{-1}$ in the presence of a $MgCl_2$ sorbent. However, from XRD it was confirmed that $Mg_3N_2$ was primarily formed, rather than $Mg(NH_3)_xCl_2$. Zeolites are also proposed as a solid sorbent for ammonia.[105,109,274] Shah *et al.*[164] reported an ammonia concentration of 3.3% at 15.5 g-$NH_3$ kW $h^{-1}$ energy yield in the presence of zeolite 5A, which is among the highest energy yields reported so far and the only reported energy yield above 10 g-$NH_3$ kW $h^{-1}$ in combination with an ammonia concentration above 1.0% (see Fig. 10). A chemical looping system based on MgO and $Mg_3N_2$ was also proposed by Zen *et al.*[295,296] Membrane reactors have also been proposed to either remove the ammonia or to feed the $H_2$ from the other side of the membrane.[144,145,297]

**4.1.2. Radiofrequency plasma reactors.** Reactors operating under radiofrequency (RF) plasma excitation have been researched to a lesser extent, as compared to DBD reactors,[261] but have recently gained substantial attention in several research groups.[190–196,298] In the late 1980s and early 1990s, Uyama *et al.* and Tanaka *et al.* used zeolite[182,187] as well as Fe[183,188] and Mo[183] wires as catalyst in the downstream of their low pressure (650 Pa) RF plasma apparatus. Fe catalysts resulted in the highest product yield. They are the only authors to report the formation of both ammonia and hydrazine[182,183,188] and speculated that the H and $NH_x$ radicals formed in the discharge are the main adsorbates.[183]

Recently, Ben Yaala *et al.*[193,195] placed W and stainless steel catalysts in their low pressure (2 Pa) RF plasma reactor. They reported the thermal decomposition of ammonia at high temperature (above 830 K on W) and the creation of stables nitrides (starting at 650 K on stainless steel), inhibiting ammonia formation.[195]

Shah *et al.*[190–192,194] placed a catalyst bed very close to the plasma electrodes in a low pressure (40 Pa) RF plasma setup. They studied various transition metal based catalysts,[191,194] Ga alloys[192,194] and a Ni–MOF (metal organic framework).[190] Within the metals, Ni and Sn based catalysts were the most active.[194] However, the Ni–MOF performed better than pure Ni, which was attributed to the porosity.[190] Ga alloys, both Ga–In[192,194] and Ga–Pd,[194] gave the best results.[192] The ammonia synthesis rate was directly correlated to the H atom radical density.[192,196] Shah *et al.*[191] also reported on modelling work, from which the mechanism for plasma-catalytic ammonia synthesis in RF reactors was disentangled. Both $N_2$ and $H_2$ dissociate in the plasma, after which N adsorbs on the surface. Subsequently, the adsorbed N atoms are hydrogenated by H atoms on the surface or in the gas phase, *i.e.*, the model revealed that both Langmuir–Hinshelwood reactions and Eley–Rideal-reactions play a role.[191]

**4.1.3. Microwave plasma reactors.** Low pressure (60–600 Pa) plasmas ignited with microwaves (MWs, *i.e.*, GHz frequency range) have received considerably less attention for ammonia synthesis compared to both RF discharges and DBDs.[261] Uyama *et al.*[181–183,189] studied MW plasmas with catalyst downstream. They found the performance of their MW plasma to be superior to their RF discharge.[182,183] Unlike the RF discharge, there was no significant hydrazine yield. This was attributed to a difference in plasma radicals created in the discharge. The RF discharge caused the adsorption of H and $NH_x$ radicals, while the MW plasma caused the adsorption of N radicals.[183] Kiyooka *et al.*[198] explored an electron cyclotron resonance plasma, which also operates within a GHz frequency range and at low pressure (600 Pa). They found that N and NH radicals adsorb onto the stainless steel reactor walls and report further hydrogenation on the surface due to H radicals in the plasma (*i.e.*, Eley–Rideal mechanism) until the desorption of ammonia.[198]

Siemsen[279] performed experiments and simulations for a MW plasma reactor with downstream Rh catalyst bed. Due to the long distance between MW plasma and catalyst, the excited $N_2$ molecules do not reach the catalytic surface, and only atomic radicals remain. Simulations revealed that the atoms account for the formed ammonia. Ammonia was not formed without catalyst.[279] Jauberteau *et al.*[184] reports that the adsorption of NH onto the stainless steel reactor walls is the first reaction step towards ammonia, from which either ammonia or adsorbed $NH_2$ is formed.

To date, only two studies considered ammonia synthesis in atmospheric pressure MW plasmas,[186,278] despite the more beneficial process conditions for industrial application. However, the highest energy yields, *i.e.*, 0.4 g-$NH_3$ kW $h^{-1}$ (see Fig. 9), have been reported for pressures as low as $10^{-4}$ bar. In addition, the reported energy yields of MW plasma reactors are orders of magnitude lower than for DBD reactors (see also Fig. 9). The reason may be that the temperatures, even downstream in the afterglow of a MW plasma, are too high for adsorption on a catalyst surface, due to (i) catalytic stability problems, but also (ii) a fundamental limitation, because adsorption always leads to loss in entropy and therefore is exothermic, implying that the equilibrium is unfavourable at very high temperatures.

**4.1.4. Glow discharges.** Various authors have researched glow discharges for ammonia synthesis over the past one and a half centuries.[170,171,173–177,264,299,300,301] Donkin reported ammonia synthesis in glow discharges as early as 1873,[264] after which Brewer *et al.* published more systematic studies with a batch process in 1929 and 1930.[170,171,299] Most research has been conducted on low-pressure glow discharges (LPGDs). In 1968 and 1969, Eremin *et al.*[300,301] considered that the wall may have an effect for ammonia synthesis, and they were the first to deliberately add catalytic materials on the reactor wall. From 1980 onward, various authors investigated a wide range of transition metals, alloys and metal oxides.[173–176,302] Coupling with catalysts is possible in glow discharges, both in a packed bed and on the walls of the reactor or the electrode.

The mechanism for ammonia synthesis from $H_2$ and $N_2$ in glow discharges has been debated over the years. Brewer

*et al.*[170] proposed that ammonia is primarily formed in the plasma phase. On the other hand, Eremin *et al.*[300,301] and Venugopalan *et al.*[173,174,176] proposed that ammonia is primarily formed on the reactor wall, which acts as a catalytic surface, as substantiated by experimental data. Venugopalan *et al.*[173,174,176] and Sugiyama *et al.*[175] proposed that N atoms are the relevant species for ammonia formation, rather than plasma-activated molecular $N_2$ species.

**4.1.5. Arc discharges.** Arc reactors such as static arc discharges and gliding arc reactors can also be used for ammonia synthesis, inspired by the commercial Birkeland–Eyde process for $NO_x$ production.[17] An advantage of gliding arcs is the scalability.[277] However, research conducted on ammonia synthesis in this type of reactor is limited.[197,201,202,303,304] Brewer *et al.*[197] first published on the application of low voltage arcs for ammonia synthesis in 1931. A detailed study on ammonia synthesis in an arc plasma was conducted by van Helden *et al.*[201,202] Implementing catalysts in arc reactors, for in-plasma catalysis, is not feasible, due to the excessive temperatures. However, post-plasma catalysis is possible, as demonstrated for other reactions, but has not yet been explored for ammonia synthesis in this type of plasma reactors.[219]

**4.1.6. Plasma–liquid systems.** Besides plasma-catalytic ammonia synthesis, ammonia has recently also been generated in plasma–liquid systems, albeit without using catalysts. In 2010, Kubota *et al.*[210] first reported ammonia synthesis in a plasma–liquid system. It is obvious that using $H_2O$ as a feedstock is more energy demanding than $H_2$.[67] On the other hand, these very simple plasma setups allow the immediate accumulation and potential storage of ammonia in $H_2O$, the most benign solvent.

A combined plasma-electrolytic system was proposed for ammonia formation from H, generated from either $H_2O$ molecules or $H^+$ ions, by Kumari *et al.*,[205] Hawtof *et al.*,[139] Haruyama *et al.*[206–209,211] and Peng *et al.*[138,140] Ammonia was formed by direct interaction of air or $N_2$ plasma with $H_2O$, allowing simpler reactors, *i.e.*, no need for counter electrodes in liquids and additional electrolysis. Gorbanev *et al.*[137] used an atmospheric pressure plasma jet with $N_2$ containing $H_2O$ vapour, in contact with liquid $H_2O$. The system offers a selectivity to ammonia of up to 96%, at energy yields up to 0.65 g-$NH_3$ kW $h^{-1}$.[137] Experiments without direct plasma–liquid interaction and with isotopically labelled water revealed the major role of $H_2O$ vapour in the feed gas, rather than liquid $H_2O$, as H-source for the ammonia synthesis.[137] There was some interaction of plasma effluent with the plasma-exposed liquid $H_2O$, but the latter decreased dramatically when $H_2O$ vapour was introduced in the $N_2$ feed gas.[137]

# 5. Mechanisms of plasma-driven ammonia synthesis

Various mechanisms are conceivable for plasma-driven ammonia synthesis, in the absence and in the presence of a catalyst. A distinction is made between plasma chemistry pathways with N atoms generated in the plasma, either reacting in the plasma phase or over the catalytic surface,[154,191] and the catalytic dissociation of excited nitrogen molecules.[96,131] This distinction is made to assess the role of the catalyst. The energy requirement of various pathways is assessed, from which we suggest that only dissociation over a catalyst (and not beforehand in the plasma phase) has the potential to become sufficiently energy efficient for practical applications. Plasma chemistry mechanisms with experimental validation are discussed. The optimal $H_2:N_2$ ratio for various mechanisms is discussed from both plasma chemistry and heterogeneous catalysis perspectives.

## 5.1. Plasma phase ammonia synthesis

The plasma phase ammonia synthesis is defined by the conversion taking place in the bulk plasma, away from the surface. In this case, the packing material does not behave as a catalyst (*i.e.*, actively contributing to the conversion process), and merely alters plasma characteristics and flow patterns in the reactor. The ammonia is formed through hydrogenation of nitrogen dissociated by the plasma.

In practice, plasma phase ammonia synthesis is difficult to disentangle from reactions on a surface, as even in the absence of packing material, the reactor walls may play a role in converting plasma-generated species on the wall.

Even though ammonia synthesis is exergonic at ambient conditions,[285] the reaction does not proceed spontaneously. Both the bonds in molecular hydrogen and molecular nitrogen need to be ruptured for ammonia formation in the gas phase. This can be accomplished by high-energy electrons in the plasma, but at the same time, these high input powers do not only affect the $N_2$ molecules but can also decompose the produced ammonia. The minimum energy requirement for ammonia formation from plasma chemistry is 66.1 MJ kg-$NH_3^{-1}$ (equivalent to 54.4 g-$NH_3$ kW $h^{-1}$), which is due to the energy required for rupturing the $N_2$ and $H_2$ bonds by the plasma (27.7 MJ kg-$NH_3^{-1}$ and 38.4 MJ kg-$NH_3^{-1}$, respectively, see Table 4). As discussed in section 4.1, the energy yield of 54.4 g-$NH_3$ kW $h^{-1}$ is too low for practical applications. This clearly shows the need for a catalyst. As shown in Table 4, only partial activation of $N_2$ by vibrational or electronic excitation may allow for a lower energy requirement. In this case, both the plasma and the catalyst have a role in the $N_2$ dissociation reaction (see section 5.3).

## 5.2. Surface-enhanced plasma-driven ammonia synthesis

In the presence of a surface, ammonia may be produced from molecular $N_2$ and $H_2$, or from plasma-generated radicals, depending on the plasma conditions and the catalytic properties of the material at a given temperature and pressure. In the current section, we discuss the conversion of plasma-generated radicals to ammonia over a catalyst, which is coined *surface-enhanced plasma-driven ammonia synthesis* (SEPDAS).[96] In section 5.3, we elaborate on the conversion of plasma-activated molecular $N_2$ to ammonia over a catalyst, which is coined *plasma-enhanced catalytic ammonia synthesis* (PECAS).[96]

 

Table 4 Energy requirements for various plasma-activations of $N_2$ and $H_2$. Partially adapted from ref. 82

| | Reaction | $N_2/H_2$-based kJ mol$^{-1}$ (eV) | $NH_3$-based MJ kg$^{-1}$ | $NH_3$-based kW h kg$^{-1}$ | $NH_3$-based g kW h$^{-1}$ |
|---|---|---|---|---|---|
| **Dissociation** | | | | | |
| $N_2$ dissociation | $N_2 + e \rightarrow 2N + e$ | 945 (9.79) | 27.7 | 7.7 | 129.8 |
| $H_2$ dissociation | $H_2 + e \rightarrow 2H + e$ | 436 (4.52) | 38.4 | 10.7 | 93.7 |
| **$N_2$ & $H_2$ dissociation** | | | **66.1** | **18.4** | **54.4** |
| **Ionization** | | | | | |
| $N_2$ ionization | $N_2 + e \rightarrow N_2^+ + e$ | 1505 (15.6) | 44.2 | 12.3 | 81.5 |
| $H_2$ ionization | $H_2 + e \rightarrow H_2^+ + e$ | 1485 (15.4) | 130.8 | 36.3 | 27.5 |
| **$N_2$ & $H_2$ ionization** | | | **175.0** | **48.6** | **20.6** |
| **Excitation** | | | | | |
| $N_2$ vibrational excitation | $N_2(X) \rightarrow N_2(X\ v = 1)$ | 28.0 (0.29) | 0.8 | 0.2 | — |
| $N_2$ electronic excitation | $N_2(X) \rightarrow N_2(A3)$ | 595.1 (6.17) | 17.5 | 4.9 | — |

If plasma-generated radicals adsorb on the catalyst surface, they can react to form ammonia. However, N, NH, and $NH_2$ radicals can also recombine to $N_2$ and $H_2$. The rate of ammonia synthesis *versus* recombination reactions towards $H_2$ and $N_2$ depends on the barriers of the relevant surface reactions on the catalyst surfaces. The number of possible surface reactions is much greater than the reactions listed in Table 1 for thermal catalysis, as these also include the reactions of all the different unique species generated in the plasma. The possible surface reactions in case of surface-enhanced plasma-driven ammonia synthesis are listed in Table 5.

It should be noted that this scheme presents a case of the second mechanism explained in section 3.5.1, *i.e.*, exploiting the plasma radicals for surface reactions other than recombination. Engelmann *et al.*[305] developed a microkinetic model for plasma-catalytic ammonia synthesis including plasma-produced N atoms, radical $NH_x$ species and vibrationally excited $N_2$. From various models it follows that the $N_2$ dissociative adsorption is no longer rate-limiting for ammonia formation. The hydrogenation reactions on the surface become rate-limiting for the ammonia formation rate, as substantiated with DFT calculations,[131,191,305] and experimental data.[191,282] In principle, the hydrogenation rate increases with decreasing nitrogen binding strength (*i.e.*, nobler catalysts). However, the $N_2$ recombination rate is also enhanced for noble catalysts.[305] This is due to a decrease in the barrier for $N_2$ recombination from 2N* for catalysts with a decreased nitrogen binding energy ($E_N$).[306] Thus, the measured activity is the result of competition between hydrogenation on the catalyst to form ammonia and recombination reactions of 2N* to form $N_2$. However, the density of H atoms in the plasma phase is typically higher than the density of N atoms, which results in a build-up of adsorbed H atoms, promoting the hydrogenation reactions. It should be noted that most transition metals do not have a barrier for $H_2$ dissociation, resulting in a high coverage of hydrogen for thermal catalysis, unless $N_2$ is dissociated at sufficient rates.[306]

DFT calculations show that Eley–Rideal-type reactions (N* + H → NH* or H* + N → NH*) may also be relevant for surface-enhanced plasma-driven ammonia synthesis,[305] due to low enthalpy barriers for these reactions (<30 kJ mol$^{-1}$).[194] In thermal catalysis, Eley–Rideal reactions are typically not considered because of entropic reasons. Stable reactant molecules would not only have to overcome the appropriate reaction barrier, they would also need to approach the active site in the right orientation and direction. In the case of plasma-generated N and H atoms, incoming angles are less important, and Engelmann *et al.*,[305] suggested by means of DFT calculations that the reactions are barrierless on all transition metals. Shah *et al.*[191] combined modelling work and experimental work, from which the authors concluded that the Eley–Rideal-like reaction H + N* → NH* is important for ammonia synthesis over an Fe catalyst in a low pressure RF plasma. The subsequent hydrogenation steps primarily occur over the Fe catalyst *via* a Langmuir–Hinshelwood mechanism,[191] while the contribution of Eley–Rideal-like mechanisms may increase with increasing plasma power and pressure. Ben Yaala *et al.*[193] performed a series of chemical looping experiments to gain insight in the mechanisms of ammonia synthesis in low pressure RF plasma on a W catalyst. They reported the highest yields for the $H_2 : N_2 = 1 : 1$ gas fraction and concluded that the Eley–Rideal reaction H + N* → NH* is a crucial step for the formation of ammonia under

Table 5 Possible surface reactions for surface-enhanced plasma-catalytic ammonia synthesis and plasma-enhanced catalytic ammonia synthesis. The * denotes an adsorption site on the catalyst

| | Reaction | Note |
|---|---|---|
| Hydrogen adsorption | $H_2 + 2* \rightleftharpoons 2H*$ | |
| | $H + * \rightleftharpoons H*$ | |
| Nitrogen adsorption | $N_2 + 2* \rightleftharpoons 2N*$ | Dominant for PECAS |
| | $N + * \rightleftharpoons N*$ | Dominant for SEPDAS |
| $NH_x$ adsorption | $NH + * \rightleftharpoons NH*$ | Dominant for SEPDAS |
| | $NH_2 + * \rightleftharpoons NH_2*$ | |
| $NH_3$ desorption | $NH_3* \rightleftharpoons NH_3 + *$ | |
| Surface hydrogenation reactions | $N* + H* \rightleftharpoons NH* + *$ | |
| | $NH* + H* \rightleftharpoons NH_2* + *$ | |
| | $NH_2* + H* \rightleftharpoons NH_3* + *$ | |
| Eley–Rideal-reactions | $N* + H \rightleftharpoons NH*$ | |
| | $NH* + H \rightleftharpoons NH_2*$ | |
| | $NH_2* + H \rightleftharpoons NH_3*$ | |
| | $H* + N \rightleftharpoons NH*$ | |
| | $H* + NH \rightleftharpoons NH_2*$ | |
| | $H* + NH_2 \rightleftharpoons NH_3*$ | |

these circumstances. It should be noted that W binds nitrogen strongly, which means that the hydrogenation steps are strongly uphill, implying it is not a typical catalyst considered for ammonia synthesis.

Hong *et al.*[82] also studied the plasma-catalytic ammonia synthesis for different plasma regimes. Their models include significantly more plasma-generated species, but with approximated values that make quantitative evaluation difficult. They concluded that mechanistically the pathways are determined by the abundant amount of H atoms adsorbed to the surface, and they propose that Eley–Rideal reactions are essential in plasma catalysis. They proposed the formation of NH in the plasma, with a subsequent NH + H* → $NH_2$* reaction, followed by hydrogenation of $NH_2$* *via* a Langmuir–Hinshelwood mechanism over the surface.

A DBD typically operates in the filamentary regime (*i.e.*, characterized by micro-discharges) when used for ammonia synthesis. Therefore, Van 't Veer *et al.*[307] developed a model explicitly considering the role of the micro-discharges and their afterglows, *i.e.* the weaker plasma in between the micro-discharges, in the ammonia formation mechanisms; see definitions in section 3.4. The calculations revealed that, while dissociative adsorption initially determines the major adsorbate, the plasma radicals, and especially the N atoms, actually determine the ammonia formation rate. Thus, electron impact dissociation of $N_2$ in the plasma, followed by N adsorption, and not $N_2$ dissociative adsorption at the catalyst surface, was identified as the rate-limiting step for ammonia formation in the DBD plasma at the conditions under study. Eley–Rideal type reactions played an overall important role, especially in the formation of NH(s). Further hydrogenation at the catalyst surface yielded ammonia. The afterglows in between the micro-discharges were found to be responsible for the net ammonia production, because during the micro-discharges ammonia is destroyed more (by electron impact dissociation) than it is formed. It should be noted that the mechanism in a DBD highly depends on the plasma and catalyst properties, as Rouwenhorst *et al.*[96] showed experimentally that the dissociative adsorption of plasma-activated $N_2$ is dominant in DBD plasmas at low energy input, while dissociation of $N_2$ in the plasma dominates at high energy input.[96,282]

Summarizing, the fraction of N, H, and $NH_x$ radicals depends on the specific energy input (SEI). In turn, the density of these plasma-generated radicals appears to determine whether Langmuir–Hinshelwood mechanisms, or Eley–Rideal-like reactions, or even plasma phase reactions are dominant.

Similar to plasma phase ammonia synthesis, the minimum energy requirement is 66.1 MJ $kg^{-1}$ in case of surface reactions with N and H atoms generated in the plasma (equivalent to 54.4 g-$NH_3$ kW $h^{-1}$, see Table 4). It should be noted that some catalysts are not able to dissociate $N_2$ at sufficient rates, while $H_2$ is readily dissociated on many metals. The minimum energy requirement in that case is 27.7 MJ $kg^{-1}$ (equivalent to 129.8 g-$NH_3$ kW $h^{-1}$, see Table 4). This is above the minimum required energy yield of 100 g-$NH_3$ kW $h^{-1}$, and potentially interesting for practical applications. It should be noted, however, that both $H_2$ and $N_2$ are activated when co-feeding both reactants, so that plasma reactor designs with primarily $N_2$ activation are required. Strategies for catalyst design for surface-enhanced plasma-driven ammonia synthesis were discussed in section 3.5.2.

### 5.3. Plasma-enhanced catalytic ammonia synthesis

Energetically, it is beneficial to prevent full dissociation of the reactants by the plasma (see Table 4). Therefore, research has recently focused on enhancing the dissociative $N_2$ adsorption on catalysts *via* vibrational or electronic excitation, following the modelling work of Mehta *et al.*[131] The authors postulated that dissociative $N_2$ adsorption is enhanced upon vibrational excitation, while the subsequent hydrogenation steps and ammonia desorption are not affected by plasma activation.[131] The authors predicted that the ammonia synthesis can be enhanced for metals that bind atomic nitrogen weakly on the catalyst surface (high $E_N$ in Fig. 11),[131] given that $N_2$ activation is usually the rate-limiting step for ammonia synthesis. This is based on microkinetic models that incorporate the potential influences of vibrational excitations in $N_2$, based on density

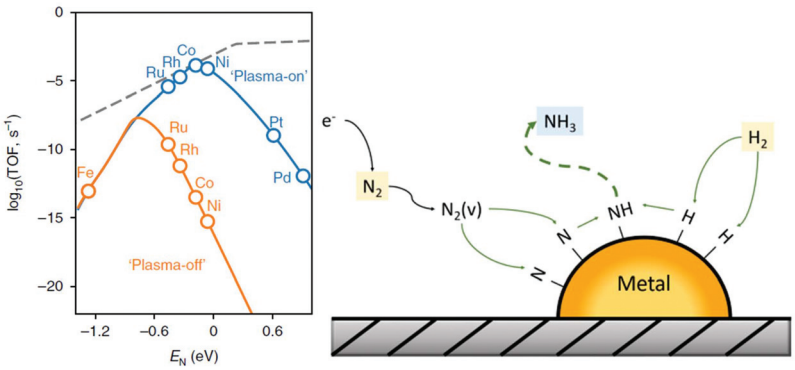


**Fig. 11** Left: Proposed effect of plasma-induced $N_2$ activation on the catalytic activity at $T$ = 200 °C and 1 bar over step sites. The dashed line represents the maximum possible hydrogenation rate. Reproduced from ref. 131. Right: Proposed mechanism for plasma-enhanced catalytic ammonia synthesis *via* plasma-activated $N_2$ dissociation. Reproduced from ref. 96.

 

functional theory (DFT) data available in literature (see Fig. 11). The vibrational energy is often not sufficient for dissociation in plasma phase, due to the large amount of energy needed to break the $N_2$ triple bond (9.79 eV), although vibrationally induced dissociation is reported for some types of plasmas.[308,309] Conversely, the energy barrier for the catalytic dissociation of $N_2$ on transition metals is considerably lower, *e.g.* 1.5 eV on Ru(111),[310] and vibrational excitation will have relatively more impact on dissociation on these metals.

Rouwenhorst *et al.*[96] substantiated this claim with a kinetic analysis for Ru-based catalysts in a DBD reactor. In case of thermal catalysis (*i.e.*, without a plasma), the apparent activation barrier of ammonia synthesis is about 60–115 kJ $mol^{-1}$, which can be attributed to the dissociation of $N_2$.[42,283] Upon plasma activation, the authors found that the apparent activation barrier for ammonia synthesis decreased to about 20–40 kJ $mol^{-1}$, which was attributed to a lower barrier for $N_2$ dissociation.[96] It is observed that the ammonia synthesis rate increases upon addition of an alkali promoter, both in thermal catalysis as well as in plasma catalysis.[96] This can be attributed to a decrease in the transition state barrier for $N_2$ dissociation in the presence of an alkali promoter due to electrostatic attractions,[40] confirming that $N_2$ dissociation is also kinetically relevant in plasma catalysis.

Proving that the catalytic activity enhancement is due to plasma-activated $N_2$ rather than plasma-generated radicals is difficult and no definitive experimental proof has been provided for transition metals other than Ru so far. Rouwenhorst *et al.*[282] found that Ru metal becomes active for ammonia synthesis below the thermal onset temperature (typically 300–400 °C[41–43,283,311]). The onset temperature for plasma catalysis is due to the desorption temperature of ammonia from Ru (typically 150–200 °C[160,312]), substantially lower than the temperature required for $N_2$ dissociation at sufficient rates (typically 300–400 °C[41–43,283,311]). Given that sufficient radicals are available for adsorption, ammonia can be formed over the metal without the need for $N_2$ dissociation on the catalyst. Rouwenhorst *et al.*[282] found that plasma-activated, molecular $N_2$ also contributes to the plasma-catalytic conversion at temperatures above 300 °C. Furthermore, the plasma-catalytic conversion to ammonia increases with the specific energy input (SEI),[165] which is due to increased plasma-activation of $N_2$.[131,282]

Another effect observed for plasma-enhanced catalytic ammonia synthesis is ammonia yields beyond the thermodynamic equilibrium limit.[282,293] Mehta *et al.*[293] developed a model for plasma-enhanced ammonia synthesis, which estimates the activities for ammonia synthesis and ammonia decomposition. The $N_2$ activation barrier is the key descriptor, while the hydrogenation steps are lumped in the model. The plasma-activation is assumed to decrease the barrier for $N_2$ dissociation and therefore increase the rate of $N_2$ dissociation. The final state of surface-adsorbed N* is assumed to be unaffected by plasma-activation of $N_2$. Upon varying the $N_2$ activation barrier, it was shown that plasma-activation can lead to ammonia synthesis beyond the thermal equilibrium. This model was experimentally validated for Ru/MgO and Ru–K/MgO catalysts.[282] Coupling the model of Mehta *et al.*[293] with experimental data, allows for distinguishing between regimes where plasma-generated radicals are dominant and regimes where plasma-activated molecular $N_2$ is dominant.[282]

As shown in Fig. 12(a), Mehta *et al.*[131] lumped the $N_2$ dissociation reaction in a single activation barrier to atomic N* on the catalyst surface, which leads to the prediction of enhancing the ammonia synthesis rate for noble catalysts with high $N_2$ activation barriers (see Fig. 11). However, $N_2$ dissociation is more complex in practice with various intermediates towards 2N* (see Fig. 12).[40,313,314] Furthermore, molecule–surface interactions may lead to energy losses upon adsorption of plasma-activated $N_2$.[315]

It remains an open question to what degree plasma-activation can lower the $N_2$ dissociation barrier for metals with a substantial barrier for $N_2$ dissociation. To account for these effects, Mehta *et al.* introduced an alpha parameter that represents the efficacy of vibrational excitation to lower the energy barrier. This alpha parameter is obtained from the Fridman–Macheret equation.[129] In reality the efficacy of vibrational excitation also depends on the degree of excitation[316–318] and it is unclear how accurate the Fridman–Macheret approximation is. To the best of our knowledge, more accurate models to describe the vibrational efficacy do not exist yet.

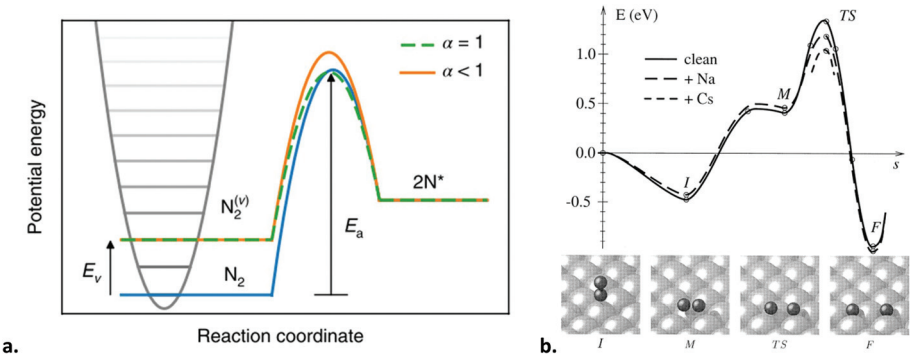


Fig. 12 (a) Proposed impact of vibrational excitation on dissociation barrier of $N_2$. Reproduced from ref. 131. (b) Minimum energy path for $N_2$ dissociation over Ru(0001), without and with alkali promoters. Reproduced from ref. 40.

## 6. Plasma-catalytic ammonia synthesis: the complexity ahead

As discussed in the previous section, plasma catalysis could become an alternative for small-scale ammonia synthesis only in two scenarios: (1) $N_2$ is dissociated by the plasma, while $H_2$ remains unaffected by the plasma, and (2) $N_2$ is only partially activated by the plasma. Some general strategies for catalyst design and for effective plasma-catalyst coupling were discussed in section 3.5. Furthermore, the possible mechanisms leading to plasma-catalytic ammonia synthesis, as well as the complexity of dissociative $N_2$ adsorption were discussed in section 5. Hereafter, we aim to shed light on potential avenues that may be relevant for the development of the field.

We want to stress that there are several known unknowns, as well as multiple unknown unknowns in plasma catalysis.[231,233] The mutual interactions between the plasma and catalyst imply that a large number of interactions may affect the plasma-driven conversions. Only recently, kinetic models were introduced in an attempt to understand plasma-catalytic ammonia synthesis in terms of the catalytic cycle.[131,191,293,305] These models have provided guidelines and concepts to interpret experimental results, but it remains difficult to link the experimental results to highly simplified models. For instance, plasma-excitations in molecular $N_2$ are predicted to shift the volcano curve to more noble metals (see Fig. 11). However, a shift to more noble metals is also to be expected for $NH_x$ radicals adsorbing and hydrogenating *via* Langmuir–Hinshelwood reactions, due to an increased hydrogenation rate over more noble metals, as well as less desorption limitations.[305] This implies both options are still open to explain catalytic trends observed in experiments. Secondly, these first models are simplifications in which not all the complexity of plasma-catalysis is incorporated, because we simply do not yet comprehend all the important contributions to plasma-catalyst interactions.[231,233] This sometimes results in disagreement between modelling results and trends observed in experiments, as discussed in section 5.3.

Specifically, the studies by Mehta *et al.*[131] and Engelmann *et al.*[305] assume specific plasma conditions that are unaffected by the catalytic reactions. Indeed, while increased TOFs were obtained by Mehta for vibrational excitations and by Engelmann for radical contributions, it is yet to be investigated whether the plasma can sustain a high vibrational temperature and high radical densities while the catalyst consumes these reactive plasma species. This, potentially, imposes limitations on the ratio of the amount of catalyst to plasma volume.

Thus, it is often difficult to distinguish between the relevant plasma species responsible for the activity enhancement in the presence of a plasma, although a few studies have strong indications for a specific pathway.[96,191,282] Based on a combined experimental and modelling study, Shah *et al.*[191] proposed that the plasma-catalytic conversion over Fe-catalysts in a low pressure RF reactor is due to dissociation of $N_2$ by the plasma, with subsequent adsorption and hydrogenation to ammonia over the surface. Based on experiments with various Ru-catalysts, Rouwenhorst *et al.*[282] showed that the plasma-enhancement over Ru-catalysts in a DBD reactor is due to reactions with $NH_x$ radicals at low temperatures (<300 °C), while plasma-activated $N_2$ with subsequent hydrogenation over the surface may also become increasingly relevant at temperatures where the activity in the absence of plasma is also substantial. Even if the activity enhancement can be proven to be due to plasma-activated $N_2$ rather than plasma-generated $NH_x$ species, it remains unresolved which plasma-activated $N_2$ species, *e.g.* with different levels of vibrational of electronic excitation, is responsible for the activity enhancement over Ru-catalysts observed in various reports.[90,96,165]

Various authors have reported an improvement in the energy efficiency for ammonia formation when using pulsed plasmas rather than AC plasmas.[158,165] For plasma-enhanced catalytic ammonia synthesis, the enhanced efficiency can be understood from the lower overall plasma power, and therefore reduced heat losses.[319] Furthermore, vibrational–translational relaxation is suppressed for pulsed plasmas,[320] thereby limiting the gas heating losses. Lastly, the electron energy distribution is different for pulsed plasmas.[321]

Jafarzadeh, Bal *et al.*[246,248,322] recently reported computational studies on enhanced surface binding of $CO_2$ on various metal cluster surfaces in case of a polarized surface; similar behavior may occur for $N_2$ binding. Surface polarization may also affect surface reactions in case of ammonia synthesis over metals, but there have not been any studies confirming or ruling out the relevance of such effects. For thermal catalysis and plasma catalysis, electrostatic attraction of alkali metals with $N_2$ cause an enhancement in $N_2$ dissociation rates.[40,96] This shows that the electronic characteristics of the catalyst are very relevant for ammonia synthesis.

Furthermore, the effect of periodic discharges and capacitive regimes is not fully understood, both on the catalytic properties of the surface[323,324] and on the plasma characteristics near the catalyst.[225,230,325] For instance, Ardagh *et al.*[323,324] reported that oscillatory surface binding strengths, induced by for instance electric fields, may enhance the catalytic activity by orders of magnitude. Furthermore, the waveform and the frequency of the oscillation can determine the catalytic activity.[323,324] As the plasma frequency and waveform is a design parameter which alters both the electron density and electron energy for $N_2$ activation in the plasma zone, as well as the catalyst surface properties, this potentially adds a new dimension to the complexity of plasma-catalytic systems.

## 7. Outlook

Over the past decades, research on plasma-catalytic ammonia synthesis has transitioned from exploratory and trial-and-error approaches to more fundamental understanding based on experimental and modelling work, as described in detail in this review paper. *Operando* plasma and catalyst diagnostics, such as surface techniques such as XPS and FTIR,[193,195] isoto-

 

pic labelling[326] and spectroscopy[194,327] will aid in further improving our understanding of how plasma and catalyst interact at the molecular level, rather than on the macroscopic level.

Open questions remain, such as which plasma-activated species are dominant for the conversion to ammonia, and under which conditions. For instance, which plasma-activated $N_2$ species is dominant for plasma-enhanced catalytic ammonia synthesis: electronically excited $N_2$ or vibrationally excited $N_2$? Furthermore, to what degree have we uncovered the complexity of plasma catalysis for plasma-driven ammonia synthesis, *i.e.* what is the role of plasma-generated radicals, and the importance of Langmuir–Hinshelwood *versus* Eley–Rideal reactions, and which unknown unknowns remain? How does the plasma environment behave very close to a metal nanoparticle on a solid surface? Additional modelling efforts may aid in enhancing the understanding.[230]

Secondly, to which degree can our understanding of plasma catalysis aid in developing sufficiently energy-efficient plasma-catalytic ammonia synthesis? Which combination of plasma reactor and catalyst leads to the highest productivity at the lowest energy cost? For now, the highest energy yields are reported for atmospheric pressure DBD reactors (see Fig. 9). On the other hand, low pressure plasma reactors such as MW and RF reactors lead to a higher degree of vibrational excitation, which may be beneficial for mild $N_2$ activation before catalytic $N_2$ dissociation. However, it should be noted that plasma activation is not the only process step for ammonia synthesis from air and water, as $H_2$ production, $N_2$ purification and ammonia separation and storage should be considered as well. The most suitable plasma reactor and catalyst are to a high degree linked to the process conditions, such as temperature and pressure for $H_2$ production, $N_2$ purification and ammonia separation and storage.

Finally, it is not yet clear whether plasma technology will be the most feasible alternative for decentralized ammonia production in the future (see Table 2). In heterogeneous catalysis, ammonia synthesis has been a guide reaction, due to the perceived simplicity of the reaction and the absence of by-products.[22,34] Thus, plasma-catalytic ammonia synthesis can certainly aid in improving our understanding of the emerging research field of plasma catalysis. Currently, plasma technology is already used for ozone production and acetylene at large scale.[328,329] Further experimental and modelling research will tell whether plasma catalysis will become a feasible alternative for green ammonia production, and whether plasma-catalytic processes will become industrially viable for other processes, like $CO_2$ and $CH_4$ conversions.[328]

## Author contributions

A. B., K. H. R. R., K. v. t. V., L. L. and Y. E. wrote section 1. A. B., K. H. R. R., K. v. t. V., L. L., R. S. P. and Y. E. co-wrote section 2. A. B., K. H. R. R., K. v. t. V., L. L. and Y. E. co-wrote section 3. A. B., K. H. R. R., K. v. t. V., L. L. and Y. E. co-wrote section 4. A. B., K. H. R. R., K. v. t. V., L. L. and Y. E. co-wrote section 5. A. B., K. H. R. R., K. v. t. V., L. L. and Y. E. co-wrote section 6. All authors reviewed the document.

## Conflicts of interest

There are no conflicts to declare.

## References

1 K. M. Van Geem, V. V. Galvita and G. B. Marin, Making chemicals with electricity, *Science*, 2019, **364**, 734–735.
2 E. Simon, Green ammonia, in *REFUEL Kickoff meeting*, 2017.
3 A. Valera-Medina, H. Xiao, M. Owen-Jones, W. I. F. David and P. J. Bowen, Ammonia for power, *Prog. Energy Combust. Sci.*, 2018, **69**, 63–102.
4 J. D. Hunt, *et al.*, Global resource potential of seasonal pumped hydropower storage for energy and water storage, *Nat. Commun.*, 2020, **11**, 947.
5 J. Guo and P. Chen, Catalyst: $NH_3$ as an Energy Carrier, *Chem*, 2017, **3**, 709–712.
6 K. H. R. Rouwenhorst, A. G. J. Van Der Ham, G. Mul and S. R. A. Kersten, Islanded ammonia power systems: Technology review & conceptual process design, *Renewable Sustainable Energy Rev.*, 2019, **114**, 109339.
7 S. Giddey, S. P. S. Badwal, C. Munnings and M. Dolan, Ammonia as a Renewable Energy Transportation Media, *ACS Sustainable Chem. Eng.*, 2017, **5**, 10231–10239.
8 V. Smil, Detonator of the population explosion, *Nature*, 1999, **400**, 415.
9 J. W. Erisman, M. A. Sutton, J. Galloway, Z. Klimont and W. Winiwarter, How a century of ammonia synthesis changed the world, *Nat. Geosci.*, 2008, **1**, 636–639.
10 M. Appl, Ammonia, 1. Introduction, *Ullmann's Encycl. Ind. Chem.*, 2011, DOI: 10.1002/14356007.a02_143.pub3.
11 M. Appl, Ammonia, 2. Production Processes, *Ullmann's Encycl. Ind. Chem.*, 2012, 295–338, DOI: 10.1002/14356007.o02_o11.
12 M. Appl, Ammonia, 3. Production Plants, *Ullmann's Encycl. Ind. Chem.*, 2012, 295–338, DOI: 10.1002/14356007.o02_o12.
13 V. Pattabathula, Ammonia, *Kirk-Othmer Encycl. Chem. Technol.*, 2019, DOI: 10.1002/0471238961.0113131503262116.a01.pub4.
14 K. H. R. Rouwenhorst, P. M. Krzywda, N. E. Benes, G. Mul and L. Lefferts, Green Ammonia Production, in *Techno-Economic Challenges of Green Ammonia as Energy Vector*, ed. R. Bañares-Alcántara and A. Valera-Medina, 2020.
15 V. Smil, *Enriching the Earth: Fritz Haber, Carl Bosch, and the Transformation of World Food Production*, 2004.
16 H. Liu, Ammonia synthesis catalyst 100 years: Practice, enlightenment and challenge, *Chin. J. Catal.*, 2014, **35**, 1619–1640.

17 B. S. Patil, Q. Wang, V. Hessel and J. Lang, Plasma $N_2$-fixation: 1900–2014, *Catal. Today*, 2015, **256**, 49–66.
18 B. S. Patil, *et al.*, Nitrogen Fixation, *Ullmann's Encycl. Ind. Chem.*, 2017, DOI: 10.1002/14356007.a17_471.pub2.
19 F. A. Ernst, *Industrial Chemical Monographs: Fixation of Atmospheric Nitrogen*, Chapman & Hall, Ltd., 1928.
20 K. H. R. Rouwenhorst, P. M. Krzywda, N. E. Benes, G. Mul and L. Lefferts, Ammonia, 4. Green Ammonia Production, *Ullmann's Encycl. Ind. Chem.*, In preparation.
21 Y. Bicer, I. Dincer, C. Zamfirescu, G. Vezina and F. Raso, Comparative life cycle assessment of various ammonia production methods, *J. Cleaner Prod.*, 2016, **135**, 1379–1395.
22 A. Hellman, K. Honkala, S. Dahl, C. H. Christensen and J. K. Nørskov, Ammonia Synthesis: State of the Bellwether Reaction, in *Comprehensive Inorganic Chemistry (II)*, Elsevier Ltd, 2013. DOI: 10.1016/B978-0-08-097774-4.00725-7.
23 R. Reimert, *et al.*, Gas Production, 2. Processes, *Ullmann's Encycl. Ind. Chem.*, 2011, 1–60, DOI: 10.1002/14356007.o12_o01.
24 T. L. Hardenburger and M. N. Ennis, Nitrogen, *Kirk-Othmer Encycl. Chem. Technol.*, 2005, 1–23, DOI: 10.1002/0471238961.1409201808011804.a01.pub2.
25 A. Sánchez and M. Martín, Scale up and scale down issues of renewable ammonia plants: Towards modular design, *Sustainable Prod. Consumption*, 2018, **16**, 176–192.
26 P. Stoltze and J. K. Nørskov, The surface science based ammonia kinetics revisited, *Top. Catal.*, 1994, **1**, 253–263.
27 P. Stoltze and J. K. Nørskov, A description of the high–pressure ammonia synthesis reaction based on surface science, *J. Vac. Sci. Technol., A*, 1987, **5**, 581–585.
28 H. Liu and W. Han, Wüstite-based catalyst for ammonia synthesis: Structure, property and performance, *Catal. Today*, 2017, **297**, 276–291.
29 J. M. Jennings, *Catalytic Ammonia Synthesis: Fundamentals and Practice*, Plenum Press, 1991.
30 A. Nielsen, *Ammonia: Catalysis and Manufacture*, Springer-Verlag, 1995.
31 H. Liu, *Ammonia Synthesis Catalysts: Innovation and Practice*, World Scientific, 2013. DOI: 10.1142/8199.
32 A. Ozaki, H. Taylor and M. Boudart, Kinetics and Mechanism of the Ammonia Synthesis, *Proc. R. Soc. A*, 1960, **258**, 47–62.
33 G. Ertl, Surface Science and Catalysis—Studies on the Mechanism of Ammonia Synthesis: The P. H. Emmett Award Address, *Catal. Rev.*, 1980, **21**, 201–223.
34 M. Boudart, Ammonia synthesis: The bellwether reaction in heterogeneous catalysis, *Top. Catal.*, 1994, **1**, 405–414.
35 J. J. Mortensen, *et al.*, Nitrogen adsorption on Fe (111), (100), and (110) surfaces, *Surf. Sci.*, 1999, **422**, 8–16.
36 J. J. Mortensen, L. B. Hansen, B. Hammer and J. K. Nørskov, Nitrogen Adsorption and Dissociation on Fe (111), *J. Catal.*, 1999, **182**, 479–488.
37 N. D. Spencer, R. C. Schoonmaker and G. A. Somorjai, Iron single crystals as ammonia synthesis catalysts: Effect of surface structure on catalyst activity, *J. Catal.*, 1982, **135**, 129–135.
38 A. Mittasch and W. Frankenburg, Early Studies of Multicomponent Catalysts, *Adv. Catal.*, 1950, **2**, 81–104.
39 E. Farber, From Chemistry to Philosophy: The Way of Alwin Mittasch (1869–1953), *Chymia*, 1966, **11**, 157–178.
40 J. J. Mortensen, B. Hammer and J. K. Nørskov, Alkali promotion of $N_2$ dissociation over Ru(0001), *Phys. Rev. Lett.*, 1998, **80**, 4333–4336.
41 K.-I. Aika, Role of alkali promoter in ammonia synthesis over ruthenium catalysts—Effect on reaction mechanism, *Catal. Today*, 2017, **286**, 14–20.
42 K.-I. Aika, A. Ohya, A. Ozaki, Y. Inoue and I. Yasumori, Support and promoter effect of ruthenium catalyst: II. Ruthenium/alkaline earth catalyst for activation of dinitrogen, *J. Catal.*, 1985, **92**, 305–311.
43 K.-I. Aika, *et al.*, Support and promoter effect of ruthenium catalyst. I. Characterization of alkali-promoted ruthenium/alumina catalysts for ammonia synthesis, *J. Catal.*, 1985, **92**, 296–304.
44 M. Kitano, *et al.*, Self-organized Ruthenium-Barium Core-Shell Nanoparticles on a Mesoporous Calcium Amide Matrix for Efficient Low-Temperature Ammonia Synthesis, *Angew. Chem., Int. Ed.*, 2018, **57**, 2648–2652.
45 M. Hara, M. Kitano and H. Hosono, Ru-Loaded C12A7:$e^-$ Electride as a Catalyst for Ammonia Synthesis, *ACS Catal.*, 2017, **7**, 2313–2324.
46 J. S. J. Hargreaves, Nitrides as ammonia synthesis catalysts and as potential nitrogen transfer reagents, *Appl. Petrochem. Res.*, 2014, **4**, 3–10.
47 C. J. H. Jacobsen, *et al.*, Catalyst Design by Interpolation in the Periodic Table: Bimetallic Ammonia Synthesis Catalysts, *J. Am. Chem. Soc.*, 2001, **123**, 8404–8405.
48 D. E. Brown, T. Edmonds, R. W. Joyner, J. J. McCarroll and S. R. Tennison, The genesis and development of the commercial BP doubly promoted catalyst for ammonia synthesis, *Catal. Lett.*, 2014, **144**, 545–552.
49 H. Liu, W. Han, C. Huo and Y. Cen, Development and application of wüstite-based ammonia synthesis catalysts, *Catal. Today*, 2019, 1–18.
50 Y. Kobayashi, M. Kitano, S. Kawamura, T. Yokoyama and H. Hosono, Kinetic evidence: The rate-determining step for ammonia synthesis over electride-supported Ru catalysts is no longer the nitrogen dissociation step, *Catal. Sci. Technol.*, 2017, **7**, 47–50.
51 Y. Inoue, *et al.*, Highly Dispersed Ru on Electride $[Ca_{24}Al_{28}O_{64}]^{4+}(e^-)_4$ as a Catalyst for Ammonia Synthesis, *ACS Catal.*, 2014, **4**(2), 674–680.
52 J. B. Hansen and P. A. Han, Roadmap to All Electric Ammonia Plants, in *NH3 Fuel Conference*, 2018.
53 J. R. Brightling, Ammonia and the fertiliser industry: The development of ammonia at Billingham, *Johnson Matthey Technol. Rev.*, 2018, **62**, 32–47.
54 European Fertilizer Manufacturers' Association, *Production of Ammonia. Best available techniques for pol-*

 

*lution prevention and control in the European fertilizer industry*, 2000.
55 Proton Ventures B. V., Sustainable ammonia for food and power, *Nitrogen + Syngas*, 2018, 1–10.
56 H. Vrijenhoef, Dutch initiatives to store sustainable energy in the form of ammonia, in *NH3 Fuel Conference*, 2017.
57 M. Reese, *et al.*, Performance of a Small-Scale Haber Process, *Ind. Eng. Chem. Res.*, 2016, **55**, 3742–3750.
58 T. Brown, *Ammonia technology portfolio: optimize for energy efficiency and carbon efficiency*, 2018.
59 E. R. Morgan, J. F. Manwell and J. G. McGowan, Sustainable Ammonia Production from U.S. Offshore Wind Farms: A Techno-Economic Review, *ACS Sustainable Chem. Eng.*, 2017, **5**, 9554–9567.
60 P. H. Pfromm, Towards sustainable agriculture: Fossil-free ammonia, *J. Renewable Sustainable Energy*, 2017, **9**, 034702.
61 M. Will, Realisation of Large-Scale Green Ammonia Plants, in *NH3 Fuel Conference*, 2018.
62 M. Will and L. Lüke, Realisation of large-scale Green Ammonia plants, in *NH3 Event*, 2018.
63 J. P. Vrijenhoef, Opportunities for small scale ammonia production, in *International Fertiliser Society*, 2017, pp. 1–16.
64 J. Schmuecker and D. Toyne, Making demonstration amounts of renewable ammonia and using it to fuel a farm tractor, in *NH3 Event*, 2019.
65 J. B. Hansen and P. Han, The SOC4NH3 Project in Denmark, in *NH3 Event*, 2019.
66 N. Cherkasov, A. O. Ibhadon and P. Fitzpatrick, A review of the existing and alternative methods for greener nitrogen fixation, *Chem. Eng. Process.*, 2015, **90**, 24–33.
67 J. G. Chen, *et al.*, Beyond fossil fuel–driven nitrogen transformations, *Science*, 2018, **360**(6391), eaar6611.
68 M. Malmali, Y. Wei, A. McCormick and E. L. Cussler, Ammonia Synthesis at Reduced Pressure via Reactive Separation, *Ind. Eng. Chem. Res.*, 2016, **55**, 8922–8932.
69 C. Philibert, Direct and indirect electrification of industry and beyond, *Oxford Rev. Econ. Policy*, 2019, **35**, 197–217.
70 Z. J. Schiffer and K. Manthiram, Electrification and Decarbonization of the Chemical Industry, *Joule*, 2017, **1**, 10–14.
71 A. Buttler and H. Spliethoff, Current status of water electrolysis for energy storage, grid balancing and sector coupling via power-to-gas and power-to-liquids: A review, *Renewable Sustainable Energy Rev.*, 2018, **82**, 2440–2454.
72 M. Carmo, D. L. Fritz, J. Mergel and D. Stolten, A comprehensive review on PEM water electrolysis, *Int. J. Hydrogen Energy*, 2013, **38**(12), 4901–4934.
73 L. Bertuccioli, *et al.*, *Development of water electrolysis in the european union: Final report*, 2014.
74 S. T. Wismann, *et al.*, Electrified methane reforming: A compact approach to greener industrial hydrogen production, *Science*, 2019, **364**, 756–759.
75 C. D. Demirhan, W. W. Tso and J. B. Powell, Sustainable Ammonia Production Through Process Synthesis and Global Optimization, *AIChE J.*, 2019, **65**(7), e16498.
76 D. Frattini, *et al.*, A system approach in energy evaluation of different renewable energies sources integration in ammonia production plants, *Renewable Energy*, 2016, **99**, 472–482.
77 A. Sánchez, M. Martín and P. Vega, Biomass Based Sustainable Ammonia Production: Digestion vs Gasification, *ACS Sustainable Chem. Eng.*, 2019, **7**, 9995–10007.
78 S. Giddey, S. P. S. Badwal and A. Kulkarni, Review of electrochemical ammonia production technologies and materials, *Int. J. Hydrogen Energy*, 2013, **38**, 14576–14594.
79 I. J. McPherson, T. Sudmeier, J. Fellowes and S. C. E. Tsang, Materials for electrochemical ammonia synthesis, *Dalton Trans.*, 2019, **48**, 1562–1568.
80 A. J. Medford and M. C. Hatzell, Photon-Driven Nitrogen Fixation: Current Progress, Thermodynamic Considerations, and Future Outlook, *ACS Catal.*, 2017, **7**, 2624–2643.
81 X. Chen, N. Li, Z. Kong, W. J. Ong and X. Zhao, Photocatalytic fixation of nitrogen to ammonia: State-of-the-art advancements and future prospects, *Mater. Horiz.*, 2018, **5**, 9–27.
82 J. Hong, S. Prawer and A. B. Murphy, Plasma Catalysis as an Alternative Route for Ammonia Production: Status, Mechanisms, and Prospects for Progress, *ACS Sustainable Chem. Eng.*, 2018, **6**, 15–31.
83 A. Bogaerts and E. C. Neyts, Plasma Technology: An Emerging Technology for Energy Storage, *ACS Energy Lett.*, 2018, **3**, 1013–1027.
84 P. Peng, *et al.*, A review on the non-thermal plasma-assisted ammonia synthesis technologies, *J. Cleaner Prod.*, 2018, **177**, 597–609.
85 T. A. Bazhenova and A. E. Shilov, Nitrogen fixation in solution, *Coord. Chem. Rev.*, 1995, **144**, 69–145.
86 J. Nørskov, *et al.*, *Sustainable Ammonia Synthesis Exploring the scientific challenges associated with discovering alternative, sustainable processes for ammonia production*, in *DOE Roundtable Report*, 2016. DOI: 10.2172/1283146.
87 W. Gao, *et al.*, Production of ammonia via a chemical looping process based on metal imides as nitrogen carriers, *Nat. Energy*, 2018, **3**, 1067–1075.
88 R. Shi, X. Zhang, G. I. N. Waterhouse, Y. Zhao and T. Zhang, The Journey toward Low Temperature, Low Pressure Catalytic Nitrogen Fixation, *Adv. Energy Mater.*, 2020, **10**(19), 2000659.
89 F. Jiao and B. Xu, Electrochemical Ammonia Synthesis and Ammonia Fuel Cells, *Adv. Mater.*, 2018, 1–5, DOI: 10.1002/adma.201805173.
90 H.-H. Kim, Y. Teramoto, A. Ogata, H. Takagi and T. Nanba, Plasma Catalysis for Environmental Treatment and Energy Applications, *Plasma Chem. Plasma Process.*, 2016, **36**, 45–72.
91 J. Hu, *et al.*, *Microwave Catalysis for Ammonia Synthesis Under Mild Reaction Conditions*, in *NH3 Fuel Conference*, 2018.

92 A. R. Singh, *et al.*, Strategies Toward Selective Electrochemical Ammonia Synthesis, *ACS Catal.*, 2019, **9**, 8316–8324.
93 L. Wang, *et al.*, Greening Ammonia toward the Solar Ammonia Refinery, *Joule*, 2018, 1–20, DOI: 10.1016/j.joule.2018.04.017.
94 CEFIC, *European chemistry for growth: Unlocking a competitive, low carbon and energy efficient future*, 2013.
95 C. Smith, A. K. Hill and L. Torrente-Murciano, Current and future role of Haber–Bosch ammonia in a carbon-free energy landscape, *Energy Environ. Sci.*, 2020, **13**(2), 331–344.
96 K. H. R. Rouwenhorst, H.-H. Kim and L. Lefferts, Vibrationally excited activation of $N_2$ in plasma-enhanced catalytic ammonia synthesis: a kinetic analysis, *ACS Sustainable Chem. Eng.*, 2019, **7**, 17515–17522.
97 K. H. R. Rouwenhorst and L. Lefferts, Feasibility study of plasma-catalytic ammonia synthesis for energy storage applications, *Catalysts*, 2020, **10**(9), 999.
98 P. Wang, *et al.*, Breaking scaling relations to achieve low-temperature ammonia synthesis through LiH-mediated nitrogen transfer and hydrogenation, *Nat. Chem.*, 2017, **9**, 64–70.
99 W. Gao, *et al.*, Barium Hydride-Mediated Nitrogen Transfer and Hydrogenation for Ammonia Synthesis: A Case Study of Cobalt, *ACS Catal.*, 2017, **7**, 3654–3661.
100 P. Wang, *et al.*, The Formation of Surface Lithium–Iron Ternary Hydride and its Function on Catalytic Ammonia Synthesis at Low Temperatures, *Angew. Chem., Int. Ed.*, 2017, **56**, 8716–8720.
101 T. Zhang, H. Miyaoka, H. Miyaoka, T. Ichikawa and Y. Kojima, Review on Ammonia Absorption Materials: Metal Hydrides, Halides, and Borohydrides, *ACS Appl. Energy Mater.*, 2018, **1**, 232–242.
102 J. W. Makepeace, *et al.*, Reversible ammonia-based and liquid organic hydrogen carriers for high-density hydrogen storage: Recent progress, *Int. J. Hydrogen Energy*, 2019, **44**, 7746–7767.
103 M. Malmali, *et al.*, Better Absorbents for Ammonia Separation, *ACS Sustainable Chem. Eng.*, 2018, **6**(5), 6536–6546.
104 M. S. Huberty, A. L. Wagner, A. McCormick and E. Cussler, Ammonia Absorption at Haber Process Conditions, *AIChE J.*, 2012, **58**, 3526–3532.
105 C. Y. Liu and K.-I. Aika, Ammonia Adsorption on Ion Exchanged Y-zeolites as Ammonia Storage Material, *J. Jpn. Pet. Inst.*, 2003, **46**, 301–307.
106 C. Y. Liu and K. Aika, Ammonia Absorption on Alkaline Earth Halides as Ammonia Separation and Storage Procedure, *Bull. Chem. Soc. Jpn.*, 2004, **77**, 123–131.
107 C. Y. Liu and K. Aika, Effect of the Cl/Br Molar Ratio of a $CaCl_2$-$CaBr_2$ Mixture Used as an Ammonia Storage Material, *Ind. Eng. Chem. Res.*, 2004, **43**, 6994–7000.
108 J. D. Beach, J. D. Kintner and A. W. Welch, Removal of gaseous $NH_3$ from an $NH_3$ reactor product stream, *US Patent*, 20180339911A1, 2018.
109 C. Y. Liu and K. Aika, Modification of active carbon and zeolite as ammonia separation materials for a new de-$NO_x$ process with ammonia on-site synthesis, *Res. Chem. Intermed.*, 2002, **28**, 409–417.
110 V. Kyriakou, I. Garagounis, E. Vasileiou, A. Vourros and M. Stoukides, Progress in the Electrochemical Synthesis of Ammonia, *Catal. Today*, 2017, **286**, 2–13.
111 K. Wang, D. Smith and Y. Zheng, Electron-driven heterogeneous catalytic synthesis of ammonia: Current states and perspective, *Carbon Resour. Convers.*, 2018, **1**, 2–31.
112 G. Soloveichik, Electrochemical synthesis of ammonia as a potential alternative to the Haber – Bosch process, *Nat. Catal.*, 2019, **2**, 377–380.
113 J. H. Montoya, C. Tsai, A. Vojvodic and J. K. Nørskov, The challenge of electrochemical ammonia synthesis: A new perspective on the role of nitrogen scaling relations, *ChemSusChem*, 2015, **8**, 2180–2186.
114 A. R. Singh, *et al.*, Electrochemical Ammonia Synthesis - The Selectivity Challenge, *ACS Catal.*, 2017, **7**, 706–709.
115 X. Cui, C. Tang and Q. Zhang, A Review of Electrocatalytic Reduction of Dinitrogen to Ammonia under Ambient Conditions, *Adv. Energy Mater.*, 2018, **8**, 1800369.
116 J. Kibsgaard, J. K. Nørskov and I. Chorkendorff, The Difficulty of Proving Electrochemical Ammonia Synthesis, *ACS Energy Lett.*, 2019, 2986–2988.
117 S. Z. Andersen, *et al.*, A rigorous electrochemical ammonia synthesis protocol with quantitative isotope measurements, *Nature*, 2019, **570**, 504–508.
118 A. R. Singh, *et al.*, Computational Design of Active Site Structures with Improved Transition-State Scaling for Ammonia Synthesis, *ACS Catal.*, 2018, **8**, 4017–4024.
119 S. L. Foster, *et al.*, Catalysts for nitrogen reduction to ammonia, *Nat. Catal.*, 2018, **1**, 490–500.
120 M. Vu, M. Sakar, S. A. Hassanzadeh-tabrizi and T. Do, Photo(electro)catalytic Nitrogen Fixation: Problems and Possibilities, *Adv. Mater. Interfaces*, 2019, **6**, 1900091.
121 U.S. Department of Energy, *Sustainable Ammonia Synthesis*, 2016.
122 J. M. McEnaney, *et al.*, Ammonia synthesis from $N_2$ and $H_2O$ using a lithium cycling electrification strategy at atmospheric pressure, *Energy Environ. Sci.*, 2017, **10**, 1621–1630.
123 P. Mehta, P. Barboun, D. B. Go, J. C. Hicks and W. F. Schneider, Catalysis Enabled by Plasma Activation of Strong Chemical Bonds: a Review, *ACS Energy Lett.*, 2019, **4**(5), 1115–1133.
124 R. Brandenburg, *et al.*, White paper on the future of plasma science in environment, for gas conversion and agriculture, *Plasma Processes Polym.*, 2018, e1700238.
125 E. C. Neyts, K. Ostrikov, M. K. Sunkara and A. Bogaerts, Plasma Catalysis: Synergistic Effects at the Nanoscale, *Chem. Rev.*, 2015, **115**, 13408–13446.
126 A. Bogaerts, *et al.*, The 2020 Plasma Catalysis Roadmap, *J. Phys. D: Appl. Phys.*, 2020, **53**, 1–51.

 

127 R. Snoeckx and A. Bogaerts, Plasma technology - a novel solution for CO2 conversion?, *Chem. Soc. Rev.*, 2017, **46**, 5805–5863.
128 A. Bogaerts, E. Neyts, R. Gijbels and J. Van Der Mullen, Gas discharge plasmas and their applications, *Spectrochim. Acta, Part B*, 2002, **57**, 609–658.
129 A. Fridman, *Plasma chemistry*, 2008.
130 R. Snoeckx and A. Bogaerts, Plasma technology – a novel solution for CO2 conversion?, *Chem. Soc. Rev.*, 2017, **46**, 5805–5863.
131 P. Mehta, *et al.*, Overcoming ammonia synthesis scaling relations with plasma-enabled catalysis, *Nat. Catal.*, 2018, **1**, 269–275.
132 Y. Uchida, K. Takaki, U. K. Urashima and J.-S. Chang, Atmospheric pressure of nitrogen plasmas in a ferro-electric packed-bed barrier discharge reactor part II: Spectroscopic measurements of excited nitrogen molecule density and its vibrational temperature, *IEEE Trans. Dielectr. Electr. Insul.*, 2004, **11**, 491–497.
133 M. Bai, Z. Zhang, M. Bai, X. Bai and H. Gao, Synthesis of Ammonia using $CH_4/N_2$ plasmas based on micro-gap discharge under environmentally friendly condition, *Plasma Chem. Plasma Process.*, 2008, **28**, 405–414.
134 M. Bai, Z. Zhang, M. Bai, X. Bai and H. Gao, Conversion of methane to liquid products, hydrogen, and ammonia with environmentally friendly condition-based microgap discharge, *J. Air Waste Manage. Assoc.*, 2008, **58**, 1616–1621.
135 M. Bai, X. Bai, N. Wang, D. Zhang and K. Zhan, Synthesis of ammonia and liquid fuel by CH4 and N2 plasmas without catalyst at ambient pressure and temperature, in *IEEE International Conference on Plasma Science*, 2004, p. 413.
136 G. Horvath, *et al.*, Packed bed DBD discharge experiments in admixtures of $N_2$ and $CH_4$, *Plasma Chem. Plasma Process.*, 2010, **30**, 565–577.
137 Y. Gorbanev, E. Vervloessem, A. Nikiforov and A. Bogaerts, Nitrogen fixation with water vapor by non-equilibrium plasma: Towards sustainable ammonia production, *ACS Sustainable Chem. Eng.*, 2020, **8**(7), 2996–3004.
138 P. Peng, *et al.*, Plasma in situ gas-liquid nitrogen fixation using concentrated high-intensity electric field, *J. Phys. D: Appl. Phys.*, 2019, **52**, 494001.
139 R. Hawtof, *et al.*, Catalyst-free, highly selective synthesis of ammonia from nitrogen and water by a plasma electrolytic system, *Asian J. Chem.*, 2019, **31**, 1–10.
140 P. Peng, *et al.*, In situ plasma-assisted atmospheric nitrogen fixation using water and spray-type jet plasma, *Chem. Commun.*, 2018, **54**, 2886–2889.
141 P. Peng, *et al.*, Sustainable non–thermal plasma–assisted nitrogen fixation – Synergistic catalysis, *ChemSusChem*, 2019, 1–12, DOI: 10.1002/cssc.201901211.
142 D. Xie, *et al.*, Ammonia synthesis and by-product formation from $H_2O$, $H_2$ and $N_2$ by dielectric barrier discharge combined with an $Ru/Al_2O_3$ catalyst, *RSC Adv.*, 2016, **6**, 105338–105346.
143 M. Bai, Z. Zhang, X. Bai, M. Bai and W. Ning, Plasma Synthesis of Ammonia With a Microgap Dielectric Barrier Discharge at Ambient Pressure, *IEEE Trans. Plasma Sci.*, 2003, **31**, 1285–1291.
144 T. Mizushima, K. Matsumoto, J. I. Sugoh, H. Ohkita and N. Kakuta, Tubular membrane-like catalyst for reactor with dielectric-barrier-discharge plasma and its performance in ammonia synthesis, *Appl. Catal., A*, 2004, **265**, 53–59.
145 T. Mizushima, K. Matsumoto, H. Ohkita and N. Kakuta, Catalytic effects of metal-loaded membrane-like alumina tubes on ammonia synthesis in atmospheric pressure plasma by dielectric barrier discharge, *Plasma Chem. Plasma Process.*, 2007, **27**, 1–11.
146 J. Hong, S. Prawer and A. B. Murphy, Production of ammonia by heterogeneous catalysis in a packed-bed dielectric-barrier discharge: Influence of argon addition and voltage, *IEEE Trans. Plasma Sci.*, 2014, **42**, 2338–2339.
147 A. Gómez-Ramírez, J. Cotrino, R. M. Lambert and A. R. González-Elipe, Efficient synthesis of ammonia from $N_2$ and $H_2$ alone in a ferroelectric packed-bed DBD reactor, *Plasma Sources Sci. Technol.*, 2015, **24**, 065011.
148 P. Peng, *et al.*, Atmospheric Pressure Ammonia Synthesis Using Non-thermal Plasma Assisted Catalysis, *Plasma Chem. Plasma Process.*, 2016, **36**, 1201–1210.
149 J. Hong, *et al.*, Plasma Catalytic Synthesis of Ammonia Using Functionalized-Carbon Coatings in an Atmospheric-Pressure Non-equilibrium Discharge, *Plasma Chem. Plasma Process.*, 2016, **36**, 917–940.
150 K. Aihara, *et al.*, Remarkable catalysis of a wool-like copper electrode for $NH_3$ synthesis from $N_2$ and $H_2$ in non-thermal atmospheric plasma, *Chem. Commun.*, 2016, **52**, 13560–13563.
151 P. Peng, *et al.*, Ru-based multifunctional mesoporous catalyst for low-pressure and non-thermal plasma synthesis of ammonia, *Int. J. Hydrogen Energy*, 2017, **42**, 19056–19066.
152 G. Akay and K. Zhang, Process intensification in ammonia synthesis using novel coassembled supported microporous catalysts promoted by nonthermal plasma, *Ind. Eng. Chem. Res.*, 2017, **56**, 457–468.
153 M. Iwamoto, M. Akiyama, K. Aihara and T. Deguchi, Ammonia Synthesis on Wool-Like Au, Pt, Pd, Ag, or Cu Electrode Catalysts in Nonthermal Atmospheric-Pressure Plasma of $N_2$ and $H_2$, *ACS Catal.*, 2017, 6924–6929.
154 J. Hong, *et al.*, Corrigendum: Kinetic modelling of $NH_3$ production in $N_2$–$H_2$ non-equilibrium atmospheric-pressure plasma catalysis, *J. Phys. D: Appl. Phys.*, 2018, **51**, 109501.
155 Q. Xie, *et al.*, Hydrogenation of plasma-excited nitrogen over an alumina catalyst for ammonia synthesis, *Int. J. Hydrogen Energy*, 2018, **43**, 14885–14891.
156 Y. Wang, *et al.*, Plasma-Enhanced Catalytic Synthesis of Ammonia over a $Ni/Al_2O_3$ Catalyst at Near-Room Temperature: Insights into the Importance of the Catalyst Surface on the Reaction Mechanism, *ACS Catal.*, 2019, **9**, 10780–10793.

157 F. Herrera, *et al.*, The impact of transition metal catalysts on macroscopic dielectric barrier discharge (DBD) characteristics in an ammonia synthesis plasma catalysis reactor, *J. Phys. D: Appl. Phys.*, 2019, **52**, 224002.
158 P. Peng, *et al.*, Atmospheric Plasma-Assisted Ammonia Synthesis Enhanced via Synergistic Catalytic Absorption, *ACS Sustainable Chem. Eng.*, 2019, **7**, 100–104.
159 P. M. Barboun, *et al.*, Distinguishing Plasma Contributions to Catalyst Performance in Plasma-Assisted Ammonia Synthesis, *ACS Sustainable Chem. Eng.*, 2019, **7**(9), 8621–8630.
160 Q. Xie, S. Zhuge, X. Song and M. Lu, Non-thermal atmospheric plasma synthesis of ammonia in a DBD reactor packed with various catalysts, *J. Phys. D: Appl. Phys.*, 2019, **53**, 064002.
161 B. S. Patil, *et al.*, Deciphering the synergy between plasma and catalyst support for ammonia synthesis in a packed dielectric barrier discharge reactor, *J. Phys. D: Appl. Phys.*, 2020, **53**, ab6a36.
162 X. Zhu, *et al.*, Ammonia synthesis over y-$Al_2O_3$ pellets in a packed-bed dielectric barrier discharge reactor, *J. Phys. D: Appl. Phys.*, 2020, **53**, 164002.
163 K. van 't Veer, F. Reniers and A. Bogaerts, Zero-dimensional modelling of unpacked and packed bed dielectric barrier discharges: The role of vibrational kinetics in ammonia synthesis, *Plasma Sources Sci. Technol.*, 2020, **29**, 045020.
164 J. R. Shah, F. Gorky, J. Lucero, M. A. Carreon and M. L. Carreon, Ammonia synthesis via atmospheric plasma- catalysis: Zeolite 5A a case of study, *Ind. Eng. Chem. Res.*, 2020, **59**, 5167–5176.
165 H.-H. Kim, Y. Teramoto, A. Ogata, H. Takagi and T. Nanba, Atmospheric-pressure nonthermal plasma synthesis of ammonia over ruthenium catalysts, *Plasma Processes Polym.*, 2017, **14**, 1–9.
166 A. Gómez-Ramírez, A. M. Montoro-Damas, J. Cotrino, R. M. Lambert and A. R. González-Elipe, About the enhancement of chemical yield during the atmospheric plasma synthesis of ammonia in a ferroelectric packed bed reactor, *Plasma Processes Polym.*, 2017, **14**, 1–8.
167 Y. Nie, *et al.*, Effect of CaO-modified $Al_2O_3$ on the synthesis of ammonia by DBD plasma, *Mod. Chem. Ind.*, 2016, **36**, 127–130.
168 G. Akay, Sustainable Ammonia and Advanced Symbiotic Fertilizer Production Using Catalytic Multi-Reaction-Zone Reactors with Nonthermal Plasma and Simultaneous Reactive Separation, *ACS Sustainable Chem. Eng.*, 2017, **5**, 11588–11606.
169 S. Li, T. van Raak and F. Gallucci, Investigating the operation parameters for ammonia synthesis in dielectric barrier discharge reactors, *J. Phys. D: Appl. Phys.*, 2020, **53**, 014008.
170 A. K. Brewer and J. W. WestHaver, The Synthesis of Ammonia in the Glow Discharge, *J. Phys. Chem.*, 1929, **33**, 883–895.
171 A. K. Brewer and J. W. Westhaver, Chemical Action in the Glow Discharge II. Further Investigation on the Synthesis of Ammonia, *J. Phys. Chem.*, 1930, **34**, 153–164.
172 E. Tiede and E. Hey, Über aktiven Stickstoff und Ammoniak-Bildung im Glimmstrom in Abhängingkeit vom Elektroden-Material unter Berücksichtigung katalytischer Probleme, *Ber. Dtsch. Chem. Ges. B*, 1933, **66**, 85–94.
173 G. Y. Botchway and M. Venugopalan, Plasma Synthesis of Ammonia in Presence of an Iron Catalyst, *Z. Phys. Chem.*, 1980, **120**, 103–110.
174 K. S. Yin and M. Venugopalan, Plasma Chemical Synthesis. I. Effect of Electrode Material on the Synthesis of Ammonia, *Plasma Chem. Plasma Process.*, 1983, **3**, 343–350.
175 K. Sugiyama, *et al.*, Ammonia synthesis by means of plasma over MgO catalyst, *Plasma Chem. Plasma Process.*, 1986, **6**, 179–193.
176 M. Touvelle, J. L. M. Licea, M. Venugopalan, J. L. Mufioz Licea and M. Venugopalan, Plasma Chemical Synthesis. II. Effect of Wall Surface on the Synthesis of Ammonia, *Plasma Chem. Plasma Process.*, 1987, **7**, 101.
177 H. Miura, *et al.*, The Formation of Ammonia in the After-Glow Region of $N_2$ Plasma, *Electrochem. Ind. Phys. Chem.*, 1988, **56**, 656–657.
178 J. Amorim, G. Baravian and G. Sultan, Absolute density measurements of ammonia synthetized in $N_2$–$H_2$ mixture discharges, *Appl. Phys. Lett.*, 1996, **68**, 1915–1917.
179 B. Gordiets, C. M. Ferreira, M. J. Pinheiro and A. Ricard, Self-consistent kinetic model of low-pressure $N_2$-$H_2$ flowing discharges: I. Volume processes, *Plasma Sources Sci. Technol.*, 1998, **7**, 363–378.
180 B. Gordiets, C. M. Ferreira, M. J. Pinheiro and A. Ricard, Self-consistent kinetic model of low-pressure $N_2$-$H_2$ flowing discharges: II. Surface processes and densities of N, H, $NH_3$ species, *Plasma Sources Sci. Technol.*, 1998, **7**, 379–388.
181 H. Uyama and O. Matsumoto, Synthesis of Ammonia in High-Frequency Discharges. II. Synthesis of Ammonia in a Microwave Discharge Under Various Conditions, *Plasma Chem. Plasma Process.*, 1989, **9**, 421–432.
182 H. Uyama and O. Matsumoto, Synthesis of ammonia in high-frequency discharges, *Plasma Chem. Plasma Process.*, 1989, **9**, 13–24.
183 S. Tanaka, H. Uyama and O. Matsumoto, Synergistic effects of catalysts and plasmas on the synthesis of ammonia and hydrazine, *Plasma Chem. Plasma Process.*, 1994, **14**, 491–504.
184 J. L. Jauberteau, I. Jauberteau and J. Aubreton, $NH_3$ and $NH_x$ < 3 radical downstream a microwave discharge sustained in an Ar-$N_2$-$H_2$ gas mixture. Study of surface reactive processes and determination of rate constants, *J. Phys. D: Appl. Phys.*, 2002, **35**, 665–674.
185 T. Fujii, K. Iwase and P. C. Selvin, Mass spectrometric analysis of a $N_2/H_2$ microwave discharge plasma, *Int. J. Mass Spectrom.*, 2002, **216**, 169–175.

 

186 J. Nakajima and H. Sekiguchi, Synthesis of ammonia using microwave discharge at atmospheric pressure, *Thin Solid Films*, 2008, **516**, 4446–4451.

187 H. Uyama, T. Uchikura, H. Niijima and O. Matsumoto, Synthesis of Ammonia with RF Discharge. Adsorption of Products on Zeolite, *Chem. Lett.*, 1987, **16**, 555–558.

188 H. Uyama, T. Nakamura, S. Tanaka and O. Matsumoto, Catalytic effect of iron wires on the syntheses of ammonia and hydrazine in a radio-frequency discharge, *Plasma Chem. Plasma Process.*, 1993, **13**, 117–131.

189 H. Uyama and O. Matsumoto, Reaction Scheme of Ammonia Formation in Microwave Discharge from Quenching Reactions of NH Radicals by Hydrogen, *Electrochem. Ind. Phys. Chem.*, 1993, **61**, 925–926.

190 J. Shah, T. Wu, J. Lucero, M. A. Carreon and M. L. Carreon, Nonthermal Plasma Synthesis of Ammonia over Ni-MOF-74, *ACS Sustainable Chem. Eng.*, 2019, **7**, 377–383.

191 J. Shah, W. Wang, A. Bogaerts and M. L. Carreon, Ammonia Synthesis by Radio Frequency Plasma Catalysis: Revealing the Underlying Mechanisms, *ACS Appl. Energy Mater.*, 2018, **1**, 4824–4839.

192 J. Shah, J. Harrison and M. Carreon, Ammonia Plasma-Catalytic Synthesis Using Low Melting Point Alloys, *Catalysts*, 2018, **8**, 437.

193 M. Ben Yaala, *et al.*, Plasma-assisted catalytic formation of ammonia in $N_2$-$H_2$ plasma on tungsten surface, *Phys. Chem. Chem. Phys.*, 2019, **21**(30), 16623–16633.

194 M. Carreon, J. Shah, F. Gorky, P. Psarras and B. Seong, Ammonia yield enhancement by hydrogen sink effect during plasma catalysis, *ChemCatChem*, 2019, **12**(4), 1200–1211.

195 M. Ben Yaala, *et al.*, Plasma-activated catalytic formation of ammonia from $N_2$–$H_2$: influence of temperature and noble gas addition, *Nucl. Fusion*, 2020, **60**, 016026.

196 M. L. Carreon, D. F. Jaramillo-Cabanzo, I. Chaudhuri, M. Menon and M. K. Sunkara, Synergistic interactions of $H_2$ and $N_2$ with molten gallium in the presence of plasma, *J. Vac. Sci. Technol., A*, 2018, **36**, 021303.

197 A. K. Brewer and R. R. Miller, The Synthesis of Ammonia in the Low Voltage Arc, *J. Am. Chem. Soc.*, 1931, **53**, 2968–2978.

198 H. Kiyooka and O. Matsumoto, Reaction scheme of ammonia synthesis in the ECR plasmas, *Plasma Chem. Plasma Process.*, 1996, **16**, 547–562.

199 M. D. Bai, *et al.*, Synthesis of ammonia in a strong electric field discharge at ambient pressure, *Plasma Chem. Plasma Process.*, 2000, **20**, 511–520.

200 P. Vankan, T. Rutten, S. Mazouffre, D. C. Schram and R. Engeln, Absolute density measurements of ammonia produced via plasma-activated catalysis, *Appl. Phys. Lett.*, 2002, **418**, 2000–2003.

201 J. H. Van Helden, *et al.*, Detailed study of the plasma-activated catalytic generation of ammonia in $N_2$-$H_2$ plasmas, *J. Appl. Phys.*, 2007, **101**, 043305.

202 J. H. Van Helden, *et al.*, Production Mechanisms of NH and $NH_2$ Radicals in $N_2$-$H_2$ Plasmas, *J. Phys. Chem. A*, 2007, **3**, 11460–11472.

203 E. Carrasco, M. Jiménez-Redondo, I. Tanarro and V. J. Herrero, Neutral and ion chemistry in low pressure dc plasmas of $H_2/N_2$ mixtures: routes for the efficient production of $NH_3$ and $NH_4^+$, *Phys. Chem. Chem. Phys.*, 2011, **13**, 19561–19572.

204 T. Body, S. Cousens, J. Kirby and C. Corr, A volume-averaged model of nitrogen – hydrogen plasma chemistry to investigate ammonia production in a plasma-surface-interaction device, *Plasma Phys. Controlled Fusion*, 2018, **60**, 075011.

205 S. Kumari, S. Pishgar, M. E. Schwarting, W. F. Paxton and J. M. Spurgeon, Synergistic plasma-assisted electrochemical reduction of nitrogen to ammonia, *Chem. Commun.*, 2018, **54**, 13347–13350.

206 T. Haruyama, *et al.*, Non-catalyzed one-step synthesis of ammonia from atmospheric air and water, *Green Chem.*, 2016, **18**, 4536–4541.

207 T. Sakakura, *et al.*, Excitation of $H_2O$ at the plasma/water interface by UV irradiation for the elevation of ammonia production, *Green Chem.*, 2018, **20**, 627–633.

208 T. Sakakura, N. Murakami, Y. Takatsuji, M. Morimoto and T. Haruyama, Contribution of Discharge Excited Atomic N, $N_2$*, and $N_2^+$ to a Plasma/Liquid Interfacial Reaction as Suggested by Quantitative Analysis, *ChemPhysChem*, 2019, **20**, 1467–1474.

209 T. Sakakura, Y. Takatsuji, M. Morimoto and T. Haruyama, Nitrogen Fixation through the Plasma/Liquid Interfacial Reaction with Controlled Conditions of Each Phase as the Reaction Locus, *Electrochemistry*, 2020, **88**, 190–194.

210 Y. Kubota, K. Koga, M. Ohno and T. Hara, Synthesis of Ammonia through Direct Chemical Reactions between an Atmospheric Nitrogen Plasma Jet and a Liquid, *Plasma Fusion Res.*, 2010, **5**, 042–042.

211 T. Sakakura, N. Murakami, Y. Takatsuji and T. Haruyama, Nitrogen Fixation in a Plasma/Liquid Interfacial Reaction and Its Switching between Reduction and Oxidation, *J. Phys. Chem. C*, 2020, **124**, 9401–9408.

212 H. Conrads and M. Schmidt, Plasma generation and plasma sources, *Plasma Sources Sci. Technol.*, 2000, **9**, 441–454.

213 C. Tendero, C. Tixier, P. Tristant, J. Desmaison and P. Leprince, Atmospheric pressure plasmas: A review, *Spectrochim. Acta, Part B*, 2006, **61**, 2–30.

214 M. Laroussi and T. Akan, Arc–Free Atmospheric Pressure Cold Plasma Jets: A Review, *Plasma Processes Polym.*, 2007, **4**, 777–788.

215 U. Ebert, *et al.*, Review of recent results on streamer discharges and discussion of their relevance for sprites and lightning, *J. Geophys. Res.*, 2010, **115**, 1–13.

216 U. Ebert, *et al.*, The multiscale nature of streamers, *Plasma Sources Sci. Technol.*, 2006, **15**, S118–S129.

217 W. Wang, H. Kim, K. Van Laer and A. Bogaerts, Streamer propagation in a packed bed plasma reactor for plasma

catalysis applications, *Chem. Eng. J.*, 2018, **334**, 2467–2479.

218 H.-H. Kim and A. Ogata, Nonthermal plasma activates catalyst: From current understanding and future prospects, *Eur. Phys. J.: Appl. Phys.*, 2011, **55**, 13806.

219 H.-H. Kim, Y. Teramoto, N. Negishi and A. Ogata, A multidisciplinary approach to understand the interactions of nonthermal plasma and catalyst: A review, *Catal. Today*, 2015, **256**, 13–22.

220 H.-H. Kim, Y. Teramoto, T. Sano, N. Negishi and A. Ogata, Effects of Si/Al ratio on the interaction of nonthermal plasma and Ag/HY catalysts, *Appl. Catal., B*, 2015, **166–167**, 9–17.

221 H.-H. Kim, Y. Teramoto and A. Ogata, Time-resolved imaging of positive pulsed corona-induced surface streamers on $TiO_2$ and $\gamma$-$Al_2O_3$ supported Ag catalysts, *J. Phys. D: Appl. Phys.*, 2016, **49**, 415204.

222 A. Mizuno and H. Ito, Basic performance of an electrostatically augmented filter consisting of a packed ferroelectric pellet layer, *J. Electrostat.*, 1990, **25**, 97–107.

223 T. Butterworth and R. W. K. Allen, Plasma-catalyst interaction studied in a single pellet DBD reactor: Dielectric constant effect on plasma dynamics, *Plasma Sources Sci. Technol.*, 2017, **26**, 065008.

224 J. Kruszelnicki, K. W. Engeling and J. E. Foster, Propagation of negative electrical discharges through 2-dimensional packed bed reactors, *J. Phys. D: Appl. Phys.*, 2017, **50**, 25203.

225 K. W. Engeling, J. Kruszelnicki and M. J. Kushner, Time-resolved evolution of micro- discharges, surface ionization waves and plasma propagation in a two-dimensional packed bed reactor, *Plasma Sources Sci. Technol.*, 2018, **27**, 085002.

226 S. Liu, L. R. Winter and J. G. Chen, Review of Plasma-Assisted Catalysis for Selective Generation of Oxygenates from $CO_2$ and $CH_4$, *ACS Catal.*, 2020, **10**(4), 2855–2871.

227 F. J. J. Peeters and M. C. M. Van de Sanden, The influence of partial surface discharging on the electrical characterization of DBDs, *Plasma Sources Sci. Technol.*, 2015, **24**, 015016.

228 E. C. Neyts and A. Bogaerts, Understanding plasma catalysis through modelling and simulation—a review, *J. Phys. D: Appl. Phys.*, 2014, **47**, 1–18.

229 E. C. Neyts, Plasma-Surface Interactions in Plasma Catalysis, *Plasma Chem. Plasma Process.*, 2016, **36**, 185–212.

230 A. Bogaerts, Q. Zhang, Y. Zhang, K. Van Laer and W. Wang, Burning questions of plasma catalysis : Answers by modeling, *Catal. Today*, 2019, **337**, 3–14.

231 J. C. Whitehead, Plasma-catalysis: Is it just a question of scale?, *Front. Chem. Sci. Eng.*, 2019, **13**, 264–273.

232 J. C. Whitehead, Plasma catalysis: A solution for environmental problems, *Pure Appl. Chem.*, 2010, **82**, 1329–1336.

233 J. C. Whitehead, Plasma-catalysis: The known knowns, the known unknowns and the unknown unknowns, *J. Phys. D: Appl. Phys.*, 2016, **49**, 243001.

234 J. C. Whitehead, Plasma-catalysis: Introduction and history, in *Plasma Catalysis: Fundamentals and Applications*, ed. X. Tu, T. Nozaki and J. C. Whitehead, Springer International Publishing AG, 2018.

235 K. Ostrikov, Plasma-nano-interface in perspective: From plasma-for-nano to nano-plasmas, *Plasma Phys. Controlled Fusion*, 2019, **61**, 014028.

236 E. C. Neyts and P. Brault, Molecular Dynamics Simulations for Plasma-Surface Interactions, *Plasma Processes Polym.*, 2017, **14**, 1–18.

237 J. Van Durme, J. Dewulf, C. Leys and H. Van Langenhove, Combining non-thermal plasma with heterogeneous catalysis in waste gas treatment: A review, *Appl. Catal., B*, 2008, **78**, 324–333.

238 B. Wang, *et al.*, The Mechanism of Non-thermal Plasma Catalysis on Volatile Organic Compounds Removal, *Catal. Surv. Asia*, 2018, **22**, 73–94.

239 K. Van Laer and A. Bogaerts, Fluid modelling of a packed bed dielectric barrier discharge plasma reactor, *Plasma Sources Sci. Technol.*, 2015, **25**, 015002.

240 K. Van Laer and A. Bogaerts, Influence of Gap Size and Dielectric Constant of the Packing Material on the Plasma Behaviour in a Packed Bed DBD Reactor: A Fluid Modelling Study, *Plasma Processes Polym.*, 2017, **14**, 1600129.

241 K. Van Laer and A. Bogaerts, How bead size and dielectric constant affect the plasma behaviour in a packed bed plasma reactor: a modelling study, *Plasma Sources Sci. Technol.*, 2017, **26**, 085007.

242 M. Liu, Y. Yi, L. Wang, H. Guo and A. Bogaerts, Hydrogenation of Carbon Dioxide to Value-Added Chemicals by Heterogeneous Catalysis and Plasma Catalysis, *Catalysts*, 2019, **9**, 275.

243 C. T. Rettner and H. Stein, Effect of vibrational energy on the dissociative chemisorption of $N_2$ on Fe(111), *J. Chem. Phys.*, 1987, **87**, 770–771.

244 J. Kim, D. B. Go and J. C. Hicks, Synergistic effects of plasma-catalyst interactions for $CH_4$ activation, *Phys. Chem. Chem. Phys.*, 2017, **19**, 13010–13021.

245 J. Quan, *et al.*, Vibration-driven reaction of $CO_2$ on Cu surfaces via Eley–Rideal-type mechanism, *Nat. Chem.*, 2019, **11**, 722–729.

246 A. Jafarzadeh, K. M. Bal, A. Bogaerts and E. C. Neyts, Activation of $CO_2$ on Copper Surfaces: The Synergy between Electric Field, Surface Morphology, and Excess Electrons, *J. Phys. Chem. C*, 2020, **124**(12), 6747–6755.

247 K. M. Bal, S. Huygh, A. Bogaerts and E. C. Neyts, Effect of plasma-induced surface charging on catalytic processes: Application to $CO_2$ activation, *Plasma Sources Sci. Technol.*, 2018, **27**, 024001.

248 K. M. Bal and E. C. Neyts, Overcoming Old Scaling Relations and Establishing New Correlations in Catalytic Surface Chemistry: Combined Effect of Charging and Doping, *J. Phys. Chem. C*, 2019, **123**, 6141–6147.

249 C. J. Lee, D. H. Lee and T. Kim, Modification of catalyst surface from interaction between catalysts and dielectric

 

barrier discharge plasma, *J. Nanosci. Nanotechnol.*, 2017, **17**, 2707–2710.

250 Y. Guo, D. Ye, K. Chen, J. He and W. Chen, Toluene decomposition using a wire-plate dielectric barrier discharge reactor with manganese oxide catalyst in situ, *J. Mol. Catal. A: Chem.*, 2006, **245**, 93–100.

251 U. Roland, F. Holzer and F. D. Kopinke, Improved oxidation of air pollutants in a non-thermal plasma, *Catal. Today*, 2002, **73**, 315–323.

252 Y. R. Zhang, K. Van Laer, E. C. Neyts and A. Bogaerts, Can plasma be formed in catalyst pores? A modeling investigation, *Appl. Catal., B*, 2016, **185**, 56–67.

253 Q. Z. Zhang and A. Bogaerts, Propagation of a plasma streamer in catalyst pores, *Plasma Sources Sci. Technol.*, 2018, **27**, 035009.

254 Y. R. Zhang, E. C. Neyts and A. Bogaerts, Influence of the material dielectric constant on plasma generation inside catalyst pores, *J. Phys. Chem. C*, 2016, **120**, 25923–25934.

255 Y. R. Zhang, E. C. Neyts and A. Bogaerts, Enhancement of plasma generation in catalyst pores with different shapes, *Plasma Sources Sci. Technol.*, 2018, **27**, 055008.

256 Q.-Z. Zhang, W.-Z. Wang and A. Bogaerts, Importance of surface charging during plasma streamer propagation in catalyst pores, *Plasma Sources Sci. Technol.*, 2018, **27**, 065009.

257 R. Kojima and K.-I. Aika, Cobalt molybdenum bimetallic nitride catalysts for ammonia synthesis, *Chem. Lett.*, 2000, **29**, 514–515.

258 T. Czerwiec, H. Michel and E. Bergmann, Low-pressure, high-density plasma nitriding: mechanisms, technology and results, *Surf. Coat. Technol.*, 1998, **108–109**, 182–190.

259 B. Ashford and X. Tu, Non-thermal plasma technology for the conversion of $CO_2$, *Curr. Opin. Green Sustainable Chem.*, 2017, **3**, 45–49.

260 E. Chiremba, K. Zhang, C. Kazak and G. Akay, Direct Nonoxidative Conversion of Methane to Hydrogen and Higher Hydrocarbons by Dielectric Barrier Discharge Plasma with Plasma Catalysis Promoters, *AIChE J.*, 2017, **63**, 4418–4429.

261 M. L. Carreon, Plasma catalytic ammonia synthesis: state of the art and future directions, *J. Phys. D: Appl. Phys.*, 2019, **52**, 483001.

262 M. Alsfeld and E. Wilhelmy, Über die Bildung von Ammoniak aus seinen Elementen durch elektrische Gasentladungen, *Ann. Phys.*, 1931, **400**, 89–123.

263 W. von Siemens, Ueber die elektrostatische Induction und die Verzögerung des Stroms in Flaschendrähten, *Ann. Phys.*, 1857, **178**, 66–122.

264 W. F. Donkin, On the direct synthesis of ammonia, *London, Edinburgh Dublin Philos. Mag. J. Sci.*, 1873, **21**, 281–282.

265 J. C. Devins and M. Burton, Formation of Hydrazine in Electric Discharge Decomposition of Ammonia, *J. Am. Chem. Soc.*, 1954, **76**, 2618–2626.

266 E. N. Eremin, A. N. Maltsev and V. L. Syaduk, Catalytic synthesis of ammonia in a barrier discharge, *Russ. J. Phys. Chem.*, 1971, **45**, 635–636.

267 L. Petitjean and A. Ricard, Emission spectroscopy study of $N_2$-$H_2$ glow discharge for metal surface nitriding, *J. Phys. D: Appl. Phys.*, 1984, **17**, 919–929.

268 J. Loureiro and A. Ricard, Electron and vibrational kinetics in an $N_2$-$H_2$ glow discharge with application to surface processes, *J. Phys. D: Appl. Phys.*, 1993, 163.

269 J. Amorim, G. Baravian and A. Ricard, Production of N, H, and NH Active Species in $N_2$-$H_2$ dc Flowing Discharges, *Plasma Chem. Plasma Process.*, 1995, **15**, 721–731.

270 P. Bletzinger and B. N. Ganguly, High fractional dissociation efficiency in $H_2$ and $H_2$-$N_2$ gas mixtures in a helical resonator discharge, *Chem. Phys. Lett.*, 1995, **247**, 584–588.

271 R. Nagpal, B. N. Ganguly, P. Bletzinger and A. Garscadden, Power deposition in H and $H_2$-$N_2$ glow discharges, *Chem. Phys. Lett.*, 1996, **257**, 386–392.

272 J. Amorim, G. Baravian, S. Bockel, A. Ricard and G. Sultan, Laser and Emission Spectroscopy in $H_2$ and $H_2$-$N_2$ dc Discharges, *J. Phys. III*, 1996, **6**, 1147–1155.

273 J. Helminen, J. Helenius, E. Paatero and I. Turunen, Adsorption Equilibria of Ammonia Gas on Inorganic and Organic Sorbents at 298.15 K, *J. Chem. Eng. Data*, 2001, **46**, 391–399.

274 J. Helminen, J. Helenius, E. Paatero and I. Turunen, Comparison of sorbents and isotherm models for $NH_3$-gas separation by adsorption, *AIChE J.*, 2000, **46**, 1541–1555.

275 C. Y. Liu and K. Aika, Ammonia Absorption into Alkaline Earth Metal Halide Mixtures as an Ammonia Storage Material, *Ind. Eng. Chem. Res.*, 2004, **43**, 7484–7491.

276 N. V. Srinath, *Plasma catalytic ammonia synthesis at atmospheric pressure in a dielectric barrier discharge reactor*, Eindhoven University of Technology, 2017.

277 B. S. Patil, *Plasma (catalyst) - assisted nitrogen fixation: reactor development for nitric oxide and ammonia production*, Eindhoven University of Technology, 2017.

278 X. Bai, *et al.*, Microwave catalytic synthesis of ammonia from methane and nitrogen, *Catal. Sci. Technol.*, 2018, **8**, 6302–6305.

279 L. G. Siemsen, *The synthesis of ammonia from hydrogen and atomic nitrogen on the Rh(110) surface*, Iowa State University, 1990.

280 M. Akiyama, K. Aihara, T. Sawaguchi, M. Matsukata and M. Iwamoto, Ammonia decomposition to clean hydrogen using non-thermal atmospheric-pressure plasma, *Int. J. Hydrogen Energy*, 2018, **43**, 14493–14497.

281 M. Bai, Z. Zhang, H. Han, Y. Wang and X. Bai, Studies of ammonia synthesis in a strong ionization discharge at ambient pressure, *Conf. Rec. Ind. Appl. Soc. IEEE-IAS Annu. Meet.*, 2001, **2**, 1103–1107.

282 K. H. R. Rouwenhorst, *et al.*, Plasma-Catalytic Ammonia Synthesis beyond Thermal Equilibrium over Ru-based Catalysts, *ChemCatChem*, 2021, under review.

283 M. Muhler, F. Rosowski, O. Hinrichsen, A. Hornung and G. Ertl, Ruthenium as catalyst for ammonia synthesis, *Stud. Surf. Sci. Catal.*, 1996, **101**, 317–326.

284 B. Hammer and J. K. Norskov, Theoretical Surface Science and Catalysis—Calculations and Concepts, *Adv. Catal.*, 2000, **45**, 71–129.
285 A. Vojvodic, *et al.*, Exploring the limits: A low-pressure, low-temperature Haber-Bosch process, *Chem. Phys. Lett.*, 2014, **598**, 108–112.
286 G. Ertl, Mechanisms of Heterogeneous Catalysis, in *Reactions at Solid Surfaces*, John Wiley & Sons, Inc., 2009, pp. 123–139.
287 Y. Yi, L. Wang, Y. Guo, S. Sun and H. Guo, Plasma-assisted ammonia decomposition over Fe–Ni alloy catalysts for COx-Free hydrogen, *AIChE J.*, 2019, **65**, 691–701.
288 L. Wang, *et al.*, Highly Dispersed Co Nanoparticles Prepared by an Improved Method for Plasma-Driven $NH_3$ Decomposition to Produce $H_2$, *Catalysts*, 2019, **9**, 107.
289 S. Q. Sun, Y. H. Yi, L. Wang, J. L. Zhang and H. C. Guo, Preparation and performance of supported bimetallic catalysts for hydrogen production from ammonia decomposition by plasma catalysis, *Acta Phys.-Chim. Sin.*, 2017, **33**, 1123–1129.
290 L. Wang, *et al.*, Synergy of DBD plasma and Fe-based catalyst in $NH_3$ decomposition: Plasma enhancing adsorption step, *Plasma Processes Polym.*, 2017, **14**, e1600111.
291 L. Wang, Y. Zhao, C. Liu, W. Gong and H. Guo, Plasma driven ammonia decomposition on a Fe-catalyst: Eliminating surface nitrogen poisoning, *Chem. Commun.*, 2013, **49**, 3787–3789.
292 L. Wang, *et al.*, $NH_3$ Decomposition for $H_2$ Generation: Effects of Cheap Metals and Supports on Plasma-Catalyst Synergy, *ACS Catal.*, 2015, **5**, 4167–4174.
293 P. Mehta, *et al.*, Plasma-Catalytic Ammonia Synthesis Beyond the Equilibrium Limit, *ACS Catal.*, 2020, **10**(12), 6726–6734.
294 H. H. Himstedt, M. S. Huberty, A. V. McCormick, L. D. Schmidt and E. L. Cussler, Ammonia synthesis enhanced by magnesium chloride absorption, *AIChE J.*, 2015, **61**, 1364–1371.
295 S. Zen, T. Abe and Y. Teramoto, Indirect Synthesis System for Ammonia from Nitrogen and Water Using Nonthermal Plasma Under Ambient Conditions, *Plasma Chem. Plasma Process.*, 2018, **38**, 347–354.
296 S. Zen, T. Abe and Y. Teramoto, Atmospheric Pressure Nonthermal Plasma Synthesis of Magnesium Nitride as a Safe Ammonia Carrier, *Plasma Chem. Plasma Process.*, 2019, **39**, 1203–1210.
297 Y. Hayakawa, *et al.*, Hydrogen production system combined with a catalytic reactor and a plasma membrane reactor from ammonia, *Int. J. Hydrogen Energy*, 2019, **44**, 9987–9993.
298 A. R. Hanna, T. L. Van Surksum and E. R. Fisher, Investigating the impact of catalysts on $N_2$ rotational and vibrational temperatures in low pressure plasmas, *J. Phys. D: Appl. Phys.*, 2019, **52**, 345202.
299 A. K. Brewer and J. W. Westhaver, Chemical Action in the Glow Discharge. IV, *J. Phys. Chem.*, 1930, **34**, 1280–1293.
300 E. N. Eremin and A. N. Maltsev, Behaviour of a catalyst in a glow-discharge plasma, *Russ. J. Phys. Chem.*, 1969, **3**, 43.
301 A. N. Maltsev and E. N. Eremin, Activity of heterogeneous catalysts in the synthesis of ammonia in the glow discharge, *Russ. J. Phys. Chem.*, 1968, **9**, 1235–1237.
302 A. de Castro and F. L. Tabarés, Role of nitrogen inventory and ion enhanced N-H recombination in the ammonia formation on tungsten walls. A DC glow discharge study, *Vacuum*, 2018, **151**, 66–72.
303 Y. Zhao, L. Wang, J. Zhang and H. Guo, Enhancing the ammonia to hydrogen (ATH) energy efficiency of alternating current arc discharge, *Int. J. Hydrogen Energy*, 2014, **39**, 7655–7663.
304 Y. Zhao, L. Wang, J. L. Zhang and H. C. Guo, Influence of non-thermal plasma discharge mode and reactor structure on ammonia decomposition to hydrogen, *Acta Phys.-Chim. Sin.*, 2014, **30**, 738–744.
305 Y. Engelmann, K. van 't Veer, E. C. Neyts, W. F. Schneider and A. Bogaerts, Plasma catalysis for ammonia synthesis: the importance of Eley-Rideal reactions, *ACS Catal.*, 2021, under revision.
306 S. Wang, *et al.*, Universal transition state scaling relations for (de)hydrogenation over transition metals, *Phys. Chem. Chem. Phys.*, 2011, **13**, 20760–20765.
307 K. Van 't Veer, Y. Engelmann, F. Reniers and A. Bogaerts, Plasma-catalytic ammonia synthesis in a DBD plasma: Role of the micro-discharges and their afterglows, *J. Phys. Chem. C*, 2021, under review.
308 W. Wang, B. Patil, S. Heijkers, V. Hessel and A. Bogaerts, Nitrogen Fixation by Gliding Arc Plasma: Better Insight by Chemical Kinetics Modelling, *ChemSusChem*, 2017, **10**, 2145–2157.
309 E. Vervloessem, M. Aghaei, F. Jardali, N. Hafezkhiabani and A. Bogaerts, Plasma-based $N_2$ fixation into $NO_x$: Insights from modeling toward optimum yields and energy costs in a gliding arc plasmatron, *ACS Sustainable Chem. Eng.*, 2020, **8**(26), 9711–9720.
310 J. S. Hummelshøj, F. Abild-pedersen, F. Studt, T. Bligaard and J. K. Nørskov, CatApp: A web application for surface chemistry and heterogeneous catalysis, *Angew. Chem., Int. Ed.*, 2012, **51**, 272–274.
311 K. Aika, *et al.*, Support and promoter effect of ruthenium catalyst. III. Kinetics of ammonia synthesis over various Ru catalysts, *Appl. Catal.*, 1986, **28**, 57–68.
312 R. Pandya, R. Mane and C. V. Rode, Cascade dehydrative amination of glycerol to oxazoline, *Catal. Sci. Technol.*, 2018, **8**, 2954–2965.
313 S. Dahl, *et al.*, Role of Steps in $N_2$ Activation on Ru(0001), *Phys. Rev. Lett.*, 1999, **83**, 1814–1817.
314 M. J. Murphy, J. F. Skelly, A. Hodgson and B. Hammer, Inverted vibrational distributions from $N_2$ recombination at Ru(001): Evidence for a metastable molecular chemisorption well, *J. Chem. Phys.*, 1999, **110**, 6954–6962.
315 L. Diekhöner, H. Mortensen and A. Baurichter, $N_2$ dissociative adsorption on Ru(0001): The role of energy loss, *J. Chem. Phys.*, 2001, **115**, 9028–9035.
316 L. B. F. Juurlink, R. R. Smith, D. R. Killelea and A. L. Utz, Comparative study of C-H stretch and bend vibrations in

 

methane activation on Ni(100) and Ni(111), *Phys. Rev. Lett.*, 2005, **94**, 208303.

317 L. B. F. Juurlink, R. R. Smith and A. L. Utz, The role of rotational excitation in the activated dissociative chemisorption of vibrationally excited methane on Ni(100), *Faraday Discuss.*, 2000, **117**, 147–160.

318 L. B. F. Juurlink, P. R. Mccabe, R. R. Smith, C. L. Dicologero and A. L. Utz, Eigenstate-resolved studies of gas-surface reactivity: $CH_4(\nu_3)$ Dissociation on Ni(100), *Phys. Rev. Lett.*, 1999, **83**, 868–871.

319 Y. Teramoto and H.-H. Kim, Effect of vibrationally excited $N_2$(v) on atomic nitrogen generation using two consecutive pulse corona discharges under atmospheric pressure $N_2$, *J. Phys. D: Appl. Phys.*, 2019, **52**, 494003, DOI: 10.1088/1361-6463/ab3f83.

320 S. Van Alphen, *et al.*, Power Pulsing to Maximize Vibrational Excitation Efficiency in $N_2$ Microwave Plasma: A Combined Experimental and Computational Study, *J. Phys. Chem. C*, 2019, **124**(3), 1765–1779.

321 G. Colonna, A. Laricchiuta and L. D. Pietanza, Time dependent selfconsistent electron energy distribution functions during nano-second repetitive discharges in reacting $N_2/H_2$ mixtures, *Plasma Phys. Controlled Fusion*, 2020, **62**, 014003.

322 A. Jafarzadeh, K. M. Bal, A. Bogaerts and E. C. Neyts, $CO_2$ Activation on $TiO_2$-Supported $Cu_5$ and $Ni_5$ Nanoclusters: Effect of Plasma-Induced Surface Charging, *J. Phys. Chem. C*, 2019, **123**, 6516–6525.

323 M. A. Ardagh, O. A. Abdelrahman and P. J. Dauenhauer, Principles of Dynamic Heterogeneous Catalysis: Surface Resonance and Turnover Frequency Response, *ACS Catal.*, 2019, **9**, 6929–6937.

324 M. A. Ardagh, T. Birol, Q. Zhang, O. A. Abdelrahman and P. J. Dauenhauer, Catalytic resonance theory: SuperVolcanoes, catalytic molecular pumps, and oscillatory steady state, *Catal. Sci. Technol.*, 2019, **9**, 5058–5076.

325 Z. Mujahid, J. Kruszelnicki, A. Hala and M. J. Kushner, Formation of surface ionization waves in a plasma enhanced packed bed reactor for catalysis applications, *Chem. Eng. J.*, 2020, **382**, 123038.

326 P. Navascués, J. M. Obrero-Pérez, J. Cotrino, A. R. González-Elipe and A. Gómez-Ramírez, Isotope labelling for reaction mechanism analysis in DBD plasma processes, *Catalysts*, 2019, **9**, 1–12.

327 A. Fateev, *et al.*, Plasma Chemistry in an Atmospheric Pressure Ar/$NH_3$ Dielectric Barrier Discharge, *Plasma Processes Polym.*, 2005, **2**, 193–200.

328 U. Kogelschatz, Dielectric Barrier Discharge: Their History, Discharge Physic, and Industrial Applications, *Plasma Chem. Plasma Process.*, 2003, **23**, 1–46.

329 P. Pässler, *et al.*, Acetylene, *Ullmann's Encycl. Ind. Chem.*, 2011, 1–50, DOI: 10.1002/14356007.a01_097.pub4.